UNIVERSIDADE ESTADUAL DE CAMPINAS

Sérgio Luis Felisbino

ASPECTOS CELULARES DA CARTILAGEM EPIFISÁRIA DE RÃS: ELEMENTOS ENVOLVIDOS NOS PROCESSOS DE CALCIFICAÇÃO E CRESCIMENTO ÓSSEO

Tese apresentada ao Instituto de Biologia para obtenção do título de Doutor em Biologia Celular e Estrutural na área de Biologia Celular.

Orientador: Prof. Dr. Hernandes Faustino de Carvalho

FICHA CATALOGRÁFICA ELABORADA PELA

BIBLIOTECA DO INSTITUTO DE BIOLOGIA – UNICAMP

Felisbino, Sérgio Luis

F335a Aspectos celulares da cartilagem epifisária de rãs: elementos envolvidos nos processos de calcificação e crescimento ósseo/Sérgio Luis Felisbino. - - Campinas, S.P.[s.n.], 2001.

84f: ilus.

Orientador: Hernandes Faustino de Carvalho

Tese (doutorado) – Universidade Estadual de Campinas. Instituto de Biologia.

1. Cartilagem. 2. Óssos. 3. Calcificação. I. Carvalho, Hernandes Faustino de.II.Universidade Estadual de Campinas.Instituto de Biologia. III. Título.

Data da Defesa: 24/05/2001

Banca Examinadora

Prof. Dr. Hernandes Faustino de Carvalho (Orientador) _____
(Assinatura)

Prof. Dr. José Mauro Granjeiro _____
(Assinatura)

Profa. Dra. Telma Maria Tenório Zorn _____
(Assinatura)

Prof. Dr. Sérgio Roberto Peres Line _____
(Assinatura)

Prof. Dr. Paulo Pinto Joazeiro _____
(Assinatura)

Prof. Dr. Celso Aparecido Bertran _____
(Assinatura)

Profa. Dra. Ivanira José Bechara _____
(Assinatura)

Dedico este trabalho

aos meus pais Valdomiro e Luiza

pelo imenso amor a mim dedicado.

À Sílvia, querida esposa,

por sua compreensão e carinho nas muitas

vezes em que este trabalho ocupou o nosso tempo.

Agradecimentos:

Ao meu orientador e amigo Hernandes, que não se limitou a apenas orientar as atividades de tese deste trabalho e não mediu esforços para que eu adquirisse uma formação mais ampla e completa. Entre tantas coisas, compartilhou generosamente sua sala de professor e me incentivou a participar de outros projetos, acreditando nas minhas capacidades de realizar este trabalho e muitos outros. Além disso, criou condições para a minha participação em atividades didáticas, na organização de um Congresso sobre Pós-Graduação, na elaboração do capítulo sobre peroxissomos no livro *A Célula 2001* e também para a realização de um estágio no exterior. A você minha eterna gratidão.

À Fundação de Amparo à Pesquisa do Estado de São Paulo – FAPESP – pelo suporte financeiro, o qual garantiu condições e tranqüilidade necessárias para a realização deste trabalho.

Ao Cesar e Renato do Ranário Atibaia pela grande colaboração, fornecendo os animais utilizados neste estudo.

Aos amigos do laboratório de matriz extracelular: Daniela, Patricia, Silvia, Helene, Jussara, Heloisa. A nossa ajuda mútua foi fundamental; a amizade é enorme e a minha saudade será constante.

Aos professores do Departamento de Biologia Celular pela excelente formação transmitida e pela agradável informalidade no convívio diário.

Aos funcionários do Departamento de Biologia Celular e aos colegas de Pós-Graduação pelas colaborações e pela convivência agradável.

Às técnicas do Laboratório de Microscopia Eletrônica do Instituto de Biologia da UNICAMP, Antônia e Adriene, pelo suporte técnico nas análises ultra-estruturais.

À Profa. Dra. Linda J. Sandell pela valiosa oportunidade de realizar um estágio em seu laboratório.

Ao Prof. Dr. Celso A. Bertran e sua equipe pela importante colaboração nas análises do material inorgânico da calcificação.

Aos professores da pré-banca, Sergio R. P. Line, Paulo P. Joazeiro e José Mauro Granjeiro, pela pronta e atenciosa leitura deste trabalho e pelas importantes sugestões para a conclusão do mesmo.

Aos novos amigos Eric e Raquel, Jenny e Bob pela acolhedora hospitalidade em Saint Louis/MO-USA.

Aos amigos Luis, Luciana, Nilda, Fabinho, Andrés, Flavia, Maria Elena, Célio, Jonas, Patricia, Adilson, Wendel, Fernanda, Sebaka e Toninho, CVX e repúblicas. Sem a amizade de vocês tudo seria mais difícil.

E, é claro, agradeço a Deus que me ama.

"Em tudo, amar e servir"
Sto. Inácio de Loyola

ÍNDICE

Resumo 09

Abstract 11

1. Introdução 13

1.1. Desenvolvimento e crescimento dos ossos longos em aves e mamíferos 14

1.2. Estrutura da cartilagem epifisária e crescimento dos ossos longos nos anfíbios anuros 15

2. Objetivos 17

3. Artigos publicados ou submetidos para publicação 18

3.1. The osteochondral ligament of *Rana catesbeiana*: a fibrous attachment between bone and articular cartilage 19

3.2. Growth cartilage calcification and the endochondral ossification in *Rana Catesbeiana* 38

3.3. Ectopic calcification of the articular cartilage in the bullfrog *Rana catesbeiana* and its possible involvement in bone closure 60

4. Considerações finais 80

5. Referências 82

Resumo

Os anfíbios anuros ocupam uma posição inferior na escala evolutiva dos vertebrados e, além disso, apresentam uma postura de repouso e um modo de locomoção bem característico. Estas características certamente influenciam a estrutura, composição e organização da matriz extracelular dos ossos, cartilagens e tendões. Estudos sobre a estrutura da cartilagem epifisária destes animais têm revelado que esta cartilagem difere em vários aspectos do modelo descrito para aves e mamíferos. As duas principais diferenças consistem na localização da cartilagem de crescimento no interior do tubo ósseo metafisário e na existência de uma expansão lateral da cartilagem articular, cobrindo a face externa da extremidade do osso periosteal. Os estudos realizados por diferentes autores sugeriram a existência de um mecanismo de crescimento ósseo menos dependente da cartilagem de crescimento e mais relacionado com a atividade dos osteoblastos no periósteo. Ou seja, o crescimento longitudinal dos ossos longos ocorre por ossificação periosteal e não por ossificação endocondral. Além disso, foram encontrados, nos anuros, sítios ectópicos de calcificação na cartilagem articular. Considerando que estas características dos anuros diferem enormemente dos modelos conhecidos para aves e mamíferos, fazia-se relevante um estudo mais detalhado sobre a estrutura da cartilagem epifisária e sobre o crescimento dos ossos longos destes animais.

Neste sentido, este projeto teve por objetivo caracterizar os aspectos celulares das diferentes regiões da cartilagem epifisária de *Rana catesbeiana* envolvidos com o crescimento ósseo e com a calcificação da cartilagem articular. Especial atenção, portanto, foi dispensada às características dos condrócitos da cartilagem de crescimento e dos osteoblastos no periósteo. Para isto, foram empregadas análises citoquímicas, citoquímicas enzimáticas, imunocitoquímicas, de incorporação de marcadores de cálcio fluorescentes e de morte celular, além de análises ultra-estruturais.

Os resultados obtidos, apresentados na forma de artigos, demonstraram que: 1) em *Rana catesbeiana,* entre a face interna da projeção lateral da cartilagem articular e a face externa da extremidade do osso periosteal, existe uma estrutura fibrosa complexa e especializada, denominado ligamento osteocondral. Este ligamento é constituído de duas regiões distintas, com células e matriz extracelular diferenciadas, exibindo um arranjo de fibras de colágeno e de células que permite a esta estrutura, ao mesmo tempo, garantir uma firme e flexível ancoragem da cartilagem articular no osso periosteal e promover o crescimento ósseo em comprimento e

espessura; 2) a ossificação endocondral é um evento tardio e não desempenha um papel essencial no desenvolvimento e crescimento dos ossos longos nestes animais. Entretanto, quando estes animais crescem e ganham peso, aparentemente, a ossificação endocondral está presente, reforçando as extremidades ósseas. Além disso, a hipertrofia e morte dos condrócitos bem como a atividade de fosfatase alcalina e a calcificação da matriz extracelular não estão diretamente associadas entre si e nem à formação de trabéculas ósseas; 3) a calcificação da cartilagem articular é um processo fisiológico nestes animais, aparecendo logo após a metamorfose e sendo estimulada por forças de compressão. Além disso, esta calcificação parece estar relacionada à formação de uma estrutura similar ao centro secundário de ossificação, encontrado nos animais com 4 anos pós-metamorfose.

Abstract

Anurans are in a lower phylogenetic position when compared to birds and mammals. Furthermore, anurans present very distinct movement and posture behavior, which obviously affect the structure, composition and organization of the extracellular matrix of tendons. Studies about the structure of anuran epiphyseal cartilage have shown that this cartilage differs in several aspects from those found in birds and mammals. The two main differences are: the growth cartilage is localized inside the bone metaphyseal tube and there is a lateral expansion of articular cartilage, covering the external surface of the periostal bone. Different authors suggested the existence of a bone growth mechanism independent of growth cartilage and more related to the osteoblasts activity on the periosteum. It means that the longitudinal growth of long bones occurs by periosteal ossification rather than by endochondral ossification. Furthermore, in the anuran, ectopic sites of calcification were found in the articular cartilage. Considering that the anuran cartilage differs of the avian and mammalian counterparts, we decided to perform a detailed study on both the epiphyseal cartilage structure and the long bone growth in these animals.

In this sense, this work characterized the cellular aspects of different regions of the epiphyseal cartilage of *Rana catesbeiana* involved with the bone growth and with articular cartilage calcification. Special attention was given to the characteristics of the growth cartilage chondrocytes and to the osteoblasts in the periosteum, using cytochemical analysis, enzymatic cytochemistry, immunocytochemistry, calcium probes, DNA fragmentation test and ultrastructural analysis.

The results showed that: 1) there is a complex and specialized fibrous attachment (the osteochondral ligament) in *Rana catesbeiana*, that anchors the inner face of the lateral articular cartilage expansion and the outer face of the periosteal bone end. This ligament has two distinct regions with different arrangements of the collagen fibers and cells, which warrant a strong and flexible anchorage of the articular cartilage to the periosteal bone, besides playing a role of periosteum and contributing to the growth of the long bones; 2) endochondral ossification is a late event and does not play an essential role in the development and growth of long bones in *R. catesbeiana*. However, as the animals grow older and gain weight, further reinforcement of the bone ends is apparently necessary and endochondral ossification takes place. Furthermore, the chondrocyte hypertrophy and death as well as alkaline phosphatase activity and matrix calcification are neither directly associated to each other nor to the formation of endochondral

bone; 3) Calcification of the articular cartilage is a non-pathological process that occurs after metamorphosis and is apparently stimulated by mechanical loading. Besides, this calcification precedes the formation of a similar structure to a secondary center of ossification of mammals, found in 4-year-old individuals.

1. Introdução

1.1 Desenvolvimento e crescimento dos ossos longos em aves e mamíferos

O desenvolvimento e crescimento dos ossos longos formados a partir de um molde cartilaginoso envolvem dois processos distintos de osteogênese.

O primeiro processo é a osteogênese periosteal (pericondral), também denominado pericondral ou cortical, no qual células do pericôndrio se diferenciam em osteoblastos e formam um colar ósseo ao redor da região mediana do molde cartilaginoso, também chamada de diáfise. Nos mamíferos, durante o crescimento ósseo pré-natal e pós-natal, a osteogênese periosteal avança em direção às extremidades ósseas, até atingir a altura da zona de cartilagem hipertrófica não calcificada, também chamada de metáfise, contudo, sem atingir as zonas de maturação e proliferação e a cartilagem articular, região também chamada de epífise. Este processo é semelhante o descrito para a ossificação intramembranosa (Gardner & Gray, 1970; Osdoby & Caplan, 1981; Bianco et al. 1998).

O segundo processo é osteogênese endocondral, na qual a cartilagem é progressivamente substituída por tecido ósseo. Esta ossificação inicia-se após a formação do colar ósseo periosteal na região diafisária do modelo cartilaginoso. Inicialmente, ocorre a invasão vascular na região do colar ósseo e da cartilagem hipertrófica não calcificada. Logo após, ocorre a formação da cavidade que abrigará a medula óssea. Desta forma, o modelo cartilaginoso começa a ser reabsorvido na diáfise e avança em direção às extremidades, metáfises e epífises.

Em uma etapa mais avançada, tem-se a formação da placa epifisária de crescimento ou cartilagem de crescimento. Nesta cartilagem, pode-se observar um arranjo colunar dos condrócitos, distribuídos em cinco diferentes zonas de cartilagem. São elas as zonas de reserva, proliferação, maturação, cartilagem hipertrófica e cartilagem hipertrófica calcificada. Esta última será constantemente reabsorvida e a matriz calcificada servirá de molde, sobre o qual osteoblastos recém-recrutados depositarão a matriz óssea (Gardner & Gray, 1970; Silvestrini et al. 1979; Osdoby & Caplan, 1981; Elerbacher et al. 1995; Cancedda et al. 1995).

Embora a ossificação periosteal não dependa de mineralização prévia e da reabsorção da cartilagem, sua progressão em direção às extremidades e conseqüente crescimento longitudinal parecem estar condicionados à ossificação endocondral, ou seja, às transformações que ocorrem na cartilagem de crescimento (Hunziker et al. 1987; Breur et al. 1991; Hunziker, 1994).

Estudos têm demonstrado que a diminuição da proliferação celular, ou da hipertrofia dos condrócitos, promove menor crescimento ósseo longitudinal e o espessamento do osso cortical (Breur et al. 1992; Barreto et al. 1993; Wilsman et al. 1996a).

Desta forma, para aves e mamíferos, está amplamente estabelecido que o crescimento ósseo longitudinal é dependente dos processos que ocorrem na cartilagem de crescimento (Barreto et al. 1993; Hunziker, 1994; Wilsman et al. 1996b).

As principais atividades desta cartilagem, envolvidas com o crescimento ósseo são a proliferação celular, a produção de matriz extracelular e a hipertrofia dos condrócitos. Além disso, existem outros fatores encontrados nas cartilagens de crescimento de aves e mamíferos que contribuem para um melhor aproveitamento destas três atividades. São eles: o arranjo colunar dos condrócitos, a sua separação longitudinal após a divisão celular e a formação de um septo longitudinal calcificado (Buckwalter et al. 1986; Hunziker & Shenk, 1989; Breur et al. 1991; Barreto et al. 1993; Hunziker 1994; Wilsman et al. 1996b).

A cartilagem de crescimento é a mais dinâmica das cartilagens, pois, além das diferentes modificações celulares, nela ocorrem também mudanças na composição da matriz extracelular ao longo das diferentes zonas. No entanto, a mudança mais marcante ocorre na matriz da zona hipertrófica. Nesta zona, os condrócitos hipertróficos sintetizam o colágeno tipo X, característico desta cartilagem. A deposição deste componente foi sugerida como um pré-requisito para os processos de mineralização da cartilagem e/ou para a invasão vascular (Schmid & Lisenmayer, 1983; Gibson & Flint, 1985; Kwan et al. 1991; Cancedda et al. 1995; Olsen 1995). Entretanto, em camundongos, verificou-se que a deleção do gene do colágeno tipo X não apresentou obstáculo para o desenvolvimento e o crescimento ósseo normais, por conseguinte, o seu envolvimento nestes processos é questionável (Rosati et al. 1994). Os condrócitos hipertróficos também secretam o pró-peptídio C-terminal do colágeno tipo II, conhecido como condrocalcina. Esta molécula também parece estar associada ao processo de mineralização da matriz da cartilagem (Poole, 1991).

Além das mudanças na composição da matriz extracelular, os condrócitos hipertróficos também apresentam atividade de fosfatase alcalina associada à membrana plasmática (Leboy et al 1989; Anderson 1995; Kirsch et al. 1997). Esta atividade, associada à produção de vesículas da matriz, é essencial para o processo de mineralização do septo longitudinal. Há também a eliminação dos condrócitos hipertróficos que, ao menos em parte, morrem por apoptose,

principalmente na zona hipertrófica calcificada, antes da invasão vascular (Kim 1995; Hatori et al. 1995; Zenmyo et al. 1996; Gibson 1998). Baseados nesta hipótese, outros autores têm sugerido que os corpos apoptóticos corresponderiam às vesículas da matriz (Kim, 1995; Hashimoto et al. 1998). Entretanto, como estas vesículas também são encontradas na zona de maturação, onde não ocorre apoptose, ainda não está completamente esclarecido se a apoptose ocorre em conseqüência da calcificação ou é um fator indutor para ela. Recentemente, foi demonstrado que condrócitos apoptóticos são reabsorvidos também por osteoclastos (Bronckers et al. 2000). Este fato tem suportado a hipótese de que o destino dos condrócitos hipertróficos é a morte por apoptose. Uma outra hipótese sugere que, sob certas circunstâncias, os condrócitos hipertróficos poderiam se desdiferenciar em células osteoblásticas e participar na produção de trabéculas ósseas (Gentili et al. 1993; Roach et al. 1995; Cancedda et al. 1995; Gerstenfeld & Shapiro, 1996). De qualquer forma, os condrócitos hipertróficos parecem desempenhar um papel essencial no processo de ossificação endocondral e, conseqüentemente, no crescimento ósseo das aves e dos mamíferos.

1.2 Estrutura da cartilagem epifisária e crescimento dos ossos longos nos anfíbios anuros

Pouco se conhece sobre a estrutura da cartilagem epifisária e os processos relacionados ao crescimento ósseo nos anfíbios em geral e em particular nos anuros.

Os anfíbios anuros ocupam uma posição inferior na escala evolutiva dos vertebrados e, além disso, apresentam uma postura de repouso e um modo de locomoção bem distinto. Estas características certamente influenciam na estrutura, composição e organização da matriz extracelular dos ossos, cartilagens e tendões (Haines, 1942; Carvalho & Felisbino, 1999; Felisbino & Carvalho, 1999).

Como nos mamíferos, o início do desenvolvimento dos ossos longos dos anuros também ocorre com a formação de um colar ósseo na região da diáfise do molde cartilaginoso. Esse osso periosteal cresce em direção às extremidades e, diferentemente do modelo de mamíferos, atinge a cartilagem articular, envolvendo externamente todas as zonas da cartilagem de crescimento, incluindo a zona de proliferação (Felisbino & Carvalho, 1999).

Nos animais adultos, persiste uma volumosa cartilagem epifisária nas extremidades ósseas. Esta cartilagem é caracterizada por seu encaixe no tubo ósseo metafisário, o que permite dividi-la em três cartilagens: a cartilagem articular, a cartilagem articular lateral e a cartilagem de

crescimento. A cartilagem articular localiza-se acima da extremidade óssea e apresenta uma expansão lateral em direção a metáfise. Esta expansão lateral, aqui denominada cartilagem articular lateral, recobre a face externa das extremidades ósseas. Entre a face interna da cartilagem articular lateral e a superfície externa do osso, existe um periósteo fibroso, rico em vasos sangüíneos. A cartilagem de crescimento encontra-se logo abaixo da cartilagem articular e internamente à extremidade do tubo ósseo (encaixada como rolha de garrafa) (Haines, 1942; Mopty & Cimarosti, 1979; Dikson, 1982; Del'Orbo et al. 1992; Felisbino & Carvalho, 1999).

A cartilagem de crescimento dos anuros possui três zonas características: a zona de proliferação, com células achatadas; a zona de maturação, com células mais arredondadas; e a zona hipertrófica, com células volumosas. Na zona de proliferação, os condrócitos dividem-se e separam-se preferencialmente na direção perpendicular em relação ao eixo longitudinal, o que difere da zona de proliferação de mamíferos, nos quais a separação das células ocorre preferencialmente na direção longitudinal. Além disso, nos anuros, as células não apresentam um arranjo colunar nítido e nem septos longitudinais definidos ou calcificados (Haines, 1942, Dikson, 1982; Del'Orbo et al. 1992; Felisbino & Carvalho, 1999). Estas características, associadas ao fato da cartilagem estar localizada internamente ao osso periosteal, levaram estes autores a concluírem que o crescimento longitudinal dos ossos longos dos anuros é, na maior parte, realizado pelo processo de ossificação periosteal. Neste caso, conseqüentemente, a cartilagem de crescimento seria responsável pela expansão do diâmetro interno das extremidades ósseas, que, com o crescimento e reabsorção da cartilagem, refletir-se-ia em maior espaço para a cavidade da medula óssea (Felisbino & Carvalho, 1999).

Nos anuros, existem também sítios ectópicos de calcificação na cartilagem articular. Estes sítios de calcificação encontram-se, principalmente, na cartilagem articular lateral e, segundo Mopty & Cimarosti (1979), que estudaram diferentes espécies de anuros, a área de cartilagem calcificada é diretamente proporcional ao tamanho ou ao peso dos animais.

Dadas estas características particulares dos anuros, pareceu-nos que uma descrição mais detalhada dos aspectos celulares das ossificações periosteal e endocondral e da calcificação da cartilagem seria de extrema importância para o entendimento destes processos nesta cartilagem e, talvez, nas epífises dos outros grupos.

2. Objetivos

2.1 Objetivo geral

Este trabalho teve por objetivo caracterizar, estrutural e ultra-estruturalmente, as diferentes regiões da cartilagem epifisária e descrever os aspectos celulares e da matriz extracelular desta cartilagem e do osso periosteal envolvidos com o crescimento dos ossos longos e com a calcificação da cartilagem articular de *Rana catesbeiana*.

2.2 Objetivos específicos:

- Caracterizar a organização celular e a constituição da matriz extracelular do periósteo localizado entre a extremidade óssea e a cartilagem articular lateral;

- Caracterizar a osteogênese periosteal e endocondral durante o crescimento dos ossos longos;

- Descrever alguns aspectos relacionados com o processo de calcificação da cartilagem articular;

- Relacionar os aspectos morfológicos encontrados nos ossos e cartilagens destes animais àqueles conhecidos para aves e mamíferos.

3. Artigos publicados ou submetidos para publicação

1. **Felisbino SL,** Carvalho HF (2000) The osteochondral ligament of *Rana catesbeiana*: a fibrous attachment between bone and articular cartilage. Tissue Cell 32: 527-536

2. **Felisbino SL,** Carvalho HF (2001) Growth cartilage calcification and the endochondral ossification in *Rana catesbeina*. Cell Tissue Research (submetido à publicação)

3. **Felisbino SL,** Carvalho HF Ectopic calcification of the articular cartilage in the bullfrog *Rana catesbeiana* and its possible involvement in bone end closure. Cell Tissue Research (submetido à publicação)

3.1. The osteochondral ligament: a fibrous attachment between bone and articular cartilage in *Rana catesbeiana*. Tissue and Cell (2000) 32: 527-536

Abstract

The anuran epiphyseal cartilage shows lateral expansion that covers the external surface of the bone, besides other features that distinguish it from the corresponding avian and mammalian structures. The fibrous structure that attachs the lateral cartilage to the bone was characterized in this work. It was designated *osteochondral ligament* (OCL) and presented two main areas. There was an inner area that was closer to the periosteal bone and contained a layer of osteoblasts and elongated cells aligned to and interspersed with thin collagen fibers. The thin processes of the cells in this area showed strong alkaline phosphatase activity. The outer area, which was closer to the cartilage, was rich in blood vessels and contained a few cells amongst thick collagen fibers. TRITC-phaloidin staining showed the cells of the inner area to be rich in F-actin, and were observed to form a net around the cell nucleus and to fill the cell processes which extended between the collagen fibers. Cells of the outer area were poor in actin cytoskeleton, while those associated with the blood vessels showed intense staining. Tubulin-staining was weak, regardless of the OCL region. The main fibers of the extracellular matrix in the OCL extended obliquely upwards from the cartilage to the bone. The collagen fibers inserted into the bone matrix as Sharpey's fibers and became progressively thicker as they made their way through the outer area to the cartilage. Immunocytochemistry showed the presence of type I and type III collagen. Microfibrils were found around the cells and amongst the collagen fibrils. These microfibrils were composed of either type VI collagen or fibrilin, as shown by immunocytochemistry. The results presented in this paper show that the osteochondral ligament of *Rana catesbeiana* is a complex and specialized fibrous attachment which guarantees a strong and flexible anchorage of the lateral articular cartilage to the periosteal bone shaft, besides playing a role in bone growth.

Introduction

The anuran epiphyseal cartilage is formed by a voluminous hyaline cartilage inserted into the end of a tubular bone. It presents distinct characteristics when compared to the avian and mammalian structures. The growth cartilage is inside the periosteal bone and the articular

cartilage presents a lateral extension covering the outer side of the periosteal bone. The epiphyseal cartilage may be divided into three regions: the articular cartilage proper, the lateral articular cartilage and the growth cartilage (for review, Felisbino & Carvalho, 1999b). Furthermore, endochondral ossification is a late event in anurans and long bone growth is dependent mostly on periosteal ossification (Haines 1942; Dickson 1982; Dell'Orbo et al. 1992; Felisbino & Carvalho 1999b).

Another interesting aspect of the anuran epiphyseal cartilage is the presence of a fibrous structure between the inner side of the lateral articular cartilage and the external surface of the periosteal bone. This fibrous tissue was assumed by others to be just a fibrous layer of the periosteum (Haines 1942, Dickson 1982; Dell'Orbo et al. 1992). We found a complex organization of cells and fibrillar components of the extracellular matrix in this area, which differs from a typical periosteum. We also identified alkaline phosphatase activity in some cells of this fibrous tissue and have suggested that it is a modified periosteum and contributes to the longitudinal and lateral growth of the long bones (Felisbino & Carvalho 1999b).

This work describes the structural and compositional aspects of this fibrous structure, which we named the osteochondral ligament (OCL). The results demonstrate that the OCL is a complex and specialized structure with an important mechanical function in the attachment of the articular cartilage to the bone shaft, besides playing a role in the elongation and thickening of the periosteal bone.

Materials and Methods

Histology

Five males and five females, 1-year-old bullfrogs (*Rana catesbeiana*) were obtained from a farm in Atibaia (São Paulo State, Brazil). The animals were killed by decapitation after cold immobilization and the distal femoral epiphyseal cartilages were dissected out and immediately fixed.

Fragments of the cartilage were fixed for 2 days in 4% formaldehyde in a phosphate buffered solution containing 0.85% NaCl. Some samples were decalcified in 4% formaldehyde, 10% acetic acid and 0.85% NaCl solution for 15 days. The material was then dehydrated in a graded ethanol series, clarified in Cedar wood oil, embedded in Paraplast-Plus embedding medium and sectioned at 6 μm. Some fragments were embedded in Polysciences JB_4 resin and

sectioned at 2 μm. Sections were stained with hematoxylin-eosin (H&E), toluidine blue (TB) or picrosirius-hematoxylin (PSH), and observed under ordinary or polarized light.

Immunocytochemistry

Paraplast sections were treated with 3% hydrogen peroxide in methanol to block the endogenous peroxidases. Those used in the immunocytochemistry for either type I or type III collagens were digested for 30 minutes with 1% pepsin in 2% acetic acid. They were then sequentially incubated with 3% BSA in PBS, the appropriate primary rabbit antibody against rat type I and type III collagen (Chemicom International Interprise, Temecula CA, USA), amino-terminal of human fibrilin-1 (Santa Cruz Biotech, Santa Cruz CA, USA) and against human type VI collagen (A gift from Eva Engvall to Kate Vogel) (Felisbino & Carvalho 1999a). They were then incubated with a peroxidase-conjugated goat anti-rabbit IgG antibody (Sigma Chemical Co., St. Louis MO, USA). The peroxidase reaction was visualised with diaminobenzidine. Sections were counter-stained with methyl green.

Alternatively, samples were frozen in liquid nitrogen, mounted in Tissue Teck, and sectioned in a Microm cryostat. Sections (7μm) were collected in silanized glass slides, fixed with cold 4% paraformaldehyde in PBS and washed with TST (Tris-buffered saline plus 0.1% Tween 20). In some instances, sections were incubated with rhodamin-phaloidin (TRITC-phalloidin, Sigma Chemical Co.) and then stained with DAPI. Other sections were blocked with 3% bovine serum albumin (BSA) in PBS for 1h at room temperature, incubated with a primary monoclonal antiboby against tubulin (CloneTUB 3.2, Sigma Chemical Co.), diluted 1:50 in a solution of 3% BSA in PBS, for 1h at room temperature. After 3x5min washes with PBS the material was then incubated with a fluorescein-conjugated goat-anti rabbit Ig (diluted 1:120, Sigma Chemical Co.) in 3% BSA in PBS. TRITC- phalloidin (25μM; Sigma Chemical Co.) was added to the secondary antibody. Sections were stained with DAPI and mounted in VectaShield (Vector Labs. Inc., Burlingane CA, USA). Some sections were stained with calcein (Sigma Chemical Co), for the localisation of the bone and calcified structures. Observations were carried out using either a Zeiss Axioskop or a Olimpus fluorescence microscope.

Enzyme histochemistry

Frozen sections were fixed with cold 4% formaldehyde in cacodylate buffer for 10 minutes, washed in the same buffer and assayed for alkaline phosphatase (AlkPase) activity using

0.1% α-naphthyl phosphate, 0.1% fast red and 50mM $MgCl_2$ in 0.1M Tris-malate buffer pH 10.0. The control was prepared using the same solution without α-naphthyl phosphate (Bancroft, 1982; Cole and Wezeman, 1987).

Transmission electron microscopy (TEM)

Selected areas of the epiphyseal cartilage were processed for TEM. Tissue fragments ($1mm^3$) were fixed with 3% glutaraldehyde plus 0.25% tannic acid in Millonig's buffer containing 0.54% glucose (Cotta-Pereira et al. 1976). Tannic acid was chosen for a better preservation and visualization of the fibrillar components. Some fragments were decalcified or not in the same solution plus 5% EDTA for 12 hours. After washing with the same buffer, the material was post-fixed with 1% osmium tetroxide, washed again, dehydrated in graded acetone, and embedded in Epon 812. Ultrathin silver sections were cut using diamond knives on a LKB ultramicrotome and contrasted with alcoholic uranyl acetate and lead citrate. Grids were examined in a Leo 906 transmission electron microscope operating at 80 kV.

Results

The epiphyseal cartilage of the distal femoral end of *R. catesbeiana* was formed by a large mass of hyaline cartilage attached to the extremity of the periosteal bone shaft and showed three regions: (1) the articular cartilage proper, (2) the lateral articular cartilage and (3) the growth cartilage. The epiphyseal cartilage was inserted into the periosteal bone and the inner surface of the lateral articular cartilage was attached to the external surface of the periosteal bone by a fibrous tissue, the osteochondral ligament (OCL) (Fig. 1).

The OCL presented two structurally distinct areas. The first one was a inner area that was close to the periosteal bone and contained two cell layers. The first one corresponded to the osteoblasts on the bone surface and the second to elongated cells oriented perpendicularly to the bone. These latter cells were highly polarized, their nuclei were positioned at a given distance from the bone and they had processes that extended towards it (Figs. 2 and 3). The outer area, close to the lateral articular cartilage, had fewer well dispersed cells and many blood vessels (Figs. 2 and 3).

AlkPase activity was concentrated in the inner area of the OCL. The reaction was associated with the processes of the elongated cells (Fig. 4).

After TRITC-phalloidin staining, a clear definition of the two areas of the OCL was found. The elongated cells of the inner area of the OCL had a flat aspect and many processes, which were filled with actin microfilaments. The cells of the outer area were poor in this cytoskeletal component. Fig. 6 is a higher magnification, showing the actin distribution in cells of the inner area. Individual actin bundles could be observed, but the limits of individual cells were hard to find. Fig. 7 shows the immunofluorescence for tubulin. Weak staining for tubulin was found. Cells of the inner region showed a marked predominance of actin, with tubulin concentrating around the cell nuclei and being excluded from the cell processes. Cells of the outer area showed some staining for tubulin, especially around the cell nuclei (Fig. 7).

Picrosirius staining revealed that the collagen fibers of the OCL extended upwards from the cartilage surface to the bone, and also showed the existence of two main organizations of the collagen fibers in the OCL (Figs. 8 and 9). Collagen fibers in the inner area were thin and inserted into the periosteal bone as Sharpey's fibers, after crossing the osteoblast layer. They were weakly birefringent, showed a green interference color and were oriented in two main directions, roughly perpendicular to each other, as they crossed the inner area of the OCL (Fig. 9)

The outer area of the OCL consisted of thick collagen fibers, which were inserted into the lateral articular cartilage and showed strong birefringence with orange to red interference colors (Figs. 8 and 9). At the transition between the two areas, the collagen fibers of the outer area fanned out and constituted the thin fibers of the inner area.

Immunocytochemistry showed a strong reaction for type I collagen in the OCL and in the bone matrix (Fig. 10). Positive reaction for type III collagen was also observed on the collagen fibers of the OCL and on the surface of the bone (Fig. 11). The immunocytochemical reaction for type VI collagen (Fig. 12 and 13) and fibrilin 1 (Fig. 14) was dispersed throughout the OCL, but concentrated on the surface of the collagen fibers close to the lateral articular cartilage.

At the edge of the lateral cartilage, a clear reorganization of the periosteal fibers was seen (Figs. 15 and 16). The periosteum on the bone surface not covered by the lateral cartilage showed collagen fibers that were aligned to the bone surface. As they reached the edge of the lateral cartilage, they followed two directions. The outermost fibers were continuous with those of the perichondrium, while the innermost fibers progressively changed direction, and became obliquely oriented with respect to the bone surface, as they constituted the OCL proper.

At the TEM, the elongated cells of the inner area of the OCL were rich in rough endoplasmic reticulum. Their cytoplasm was stretched and undulated and showed long and numerous processes. These processes established connections between adjacent cells and also surrounded groups of collagen fibrils, organizing them in fibers (Fig. 17). Figure 18 is a detail of the cell processes showing that they were filled with microfilaments and showing their intimate contact with collagen fibrils. These collagen fibrils were crossed in different patterns.

Figure 19 is an aspect of the OCL to bone transition. The collagen fibers of the OCL inserted obliquely into the mineralized bone matrix. Osteoblasts were intimately associated with the bone surface and with the OCL fibers as well.

In the outer area of the OCL, the collagen fibrils were organized into thick and wavy collagen fibers (Fig. 20). Cells in this area were typical fibroblasts (Fig. 20) or differed from them by showing an abundant cytoplasm filled with rough endoplasmic reticulum and secretory vesicles, besides mitochondria and cytoskeletal components (Fig. 21). Besides collagen fibrils, the extracellular matrix in this area also exhibited microfibrils that were found around the cells and amongst the collagen fibrils (Fig. 22). In some instances the microfibrils formed bundles, which were found on the surface of the collagen fibers (Fig. 23).

Discussion

The epiphyseal cartilage of *Rana catesbeiana* shows distinct structural features as compared to its mammalian and avian counterparts (Felisbino & Carvalho 1999b). It is inserted at the end of a tubular bone and, given the absence of any endochondral bone up to the adult stage, the attachment of the cartilage to the bone is essentially provided by the anchorage of the lateral articular cartilage to the outer surface of the bone, through a specialized fibrous structure, the osteochondral ligament.

In contrast, the adult articular cartilage in mammals is a thin layer of cartilaginous tissue at the end of the long bones. It is firmly attached to bone through a calcified transition zone. Laterally, it shows fibrous connections to the periosteum at the Ranvier's groove (Speer 1982; Elerbacher et al. 1995).

Striking similarity exists between the osteochondral ligament of the bullfrog epiphyseal cartilage and the periodontal ligament. Similarly, the fiber distribution in the two structures

establishes a firm connection between structures, with rather distinct material properties, besides allowing relative movement between them.

The fibers of the periodontal ligament run obliquely upwards from the cementum to the bone, so that pressure on the tooth applies tension to the fibers inserted into the bone (Fawcett 1994). Likewise, pressure on the lateral cartilage exerts tension on the fibers of the OCL.

The wavy or crimped structure of the collagen fibers demonstrates that they are capable of some stretching (Carvalho & Vidal 1994), reinforcing the hypothesis that relative movement occurs between the lateral cartilage and the periosteal bone.

Collagen fibers in the OCL are composed of type I and III collagens. They were differently organized in each area of the OCL, being thick at the insertion into the cartilage and thinner at the transition to the bone. A transition zone, in some aspects similar to the intermediate plexus of the periodontal ligament, marks the changes in collagen fiber organization. In this zone, the thick fibers of the outermost area fan out and extend into the innermost area as thin fibers between the elongated cells (*ca* in figure 8). After crossing the highly cellular area and the ostoblastic cell layer, they inserted into the bone. Since these fibers are collagenous in nature and run perpendicular or slightly obliquely to the bone and are probably responsible for the attachment of the OCL (and eventually of the lateral articular cartilage) to the bone, they may be classified as Sharpey's fibers.

The reason for the modifications in fiber organization in the OCL is not clear, but they may represent a mechanism to disperse load throughout the bone matrix, besides associating an anchoring function to the high metabolic activities of the cells in this area.

Type VI collagen and fibrilin 1 are the major proteins of distinct types of extracellular matrix microfibrils. Both of them were found in association with collagen fibers of the OCL. Type VI microfibrils were suggested to play a major role in the organization and integration of the collagen fibers in a coordinated system (Bruns et al. 1986; Keene et al. 1988).

In addition, fibrillin based microfibrils are extensible and seem to guarantee relative distensibility to the tissues (Keene et al. 1991). While the accumulation of collage type VI microfibrils in the outer area of the OCL may represent a mechanism to fill up and organize the spaces between the thicker collagen fibers in this area, the fibrilin-based microfibrils are probably related to the arrangement of the collagen fibers, as discussed earlier (Carvalho & Vidal,1995).

We have shown before (Felisbino & Carvalho 1999b) and confirmed here, that cells of the inner area of the OCL (adjacent to the bone surface) express alkaline phosphatase activity and probably play a role in the formation and growth of the bone. Furthermore, by using TRITC-phalloiding staining, we showed a clear delimitation of this inner area. The processes of the elongated cells in the inner area of the OCL were filled with actin microfilaments, as observed by TEM, and they were clearly seen by fluorescence microscopy of the TRITC-phalloidin stained sections. The elongated cells were also rich in rough endoplasmic reticulum, demonstrating their high synthetic activity.

While attaching the lateral cartilage to the bone is a clear function of the OCL, its participation in other epiphyseal functions is not known. The aspects of fibrillar and cellular organization in the innermost area of the OCL are indicatives that they are metabolically active and that, besides taking part in the turnover of the OCL components, they are probably associated with the thickening of the periosteal bone.

The rich blood vessel supply found in the OCL reinforces the idea that its cells are metabolically active.

It seems worth mentioning that the OCL is formed by proliferation of the cells at the tip of the periosteal bone, where the two areas described here are not so well defined. However, this area will be the focus of another publication.

In conclusion, the osteochondral ligament of *R. catesbeiana* is a specialised periosteum, functioning in the anchorage of the lateral articular cartilage to the bone shaft, besides playing an active role in the growth of the long bones.

The OCL results from the existence of the lateral cartilage, which was suggested (Felisbino and Carvalho, 1999b) to be an adaptation to the high amplitude of movements expected to occur during swimming and jumping, and also to the characteristic resting position, in which the knees are kept bent. In this way, the lateral articular cartilage is under greater loading than the articular cartilage proper.

References

Bancroft, J.D. 1982. Enzyme histochemistry. In Theory and Practice of Histological Techniques (eds J. D. Bancroft and A. Stevens). Edinburgh: Churchill Livingstone.

Bruns, R.R., Press, W., Engvall, E., Timpl, R. and Gross, J. 1986. Type VI collagen in extracellular, 100-nm periodic filaments and fibrils: identification by immunoelectron microscopy. J. Cell Biol., 103, 393-404.

Carvalho, H.F., Vidal, B.C. 1994. The unique fibrillar arrangement of the bullfrog pressure-bearing tendon as an indicative of great functional deformability. Biol. Cell., 82, 59-65.

Carvalho, H.F., Vidal, B. C. 1995. The elastic system of a pressure bearing tendon of the bullfrog. Ann.Anat., *177:* 397-404.

Cole, A.A. and Wezeman, F.H. 1987. Cytochemical localization of tartrate-resistant acid phosphatase, alkaline phosphatase, and nonspecific esterase in perivascular cells of cartilage canals in the developing mouse epiphysis. Am. J. Anat., 180, 237-242.

Cotta-Pereira, G., Rodrigo, F.G. and David-Ferreira, J.F. 1976. The use of tannic acid-glutaraldehyde in the study of elastic related fibers. Stain Technol., 51, 7-11.

Dell'Orbo, C., Gioglio, L. and Quacci, D. 1992. Morphology of epiphyseal apparatus of a ranid frog. Histol. Histopathol., 7, 267-273.

Dikson, R.G. 1982. Ultrastruture of growth cartilage in the proximal femur of the frog, *Rana temporaria*. J. Anat., 135, 549-564.

Elerbacher, A., Filvaroff, E.H., Giltelman, S.E. and Derynck, R. 1995. Toward a molecular understanding of skeletal development. Cell, 80, 371-378.

Fawcett, D.W. 1994. A text book of histology. 12th. Ed. Chapman & Hall, New York.

Felisbino, S.L., Carvalho HF. 1999a. Identification and distribution of type VI collagen in tendon fibrocartilages. J . Submicrosc. Cytol. Pathol., 31, 187-185.

Felisbino, S.L., Carvalho, H.F. 1999b. The epiphyseal cartilage and growth of long bones in *Rana catesbeiana*. Tissue Cell, 31, 301-307.

Haines, R.W. 1942. The evolution of epiphyses and of endochondral bone. Biol. Rev., 17, 267-292.

Keene, D.R. Engvall, E. and Glanville R.W. 1988. The ultrastructure of type VI collagen in human skin and cartilage suggests an anchoring function for this filamentous network. J. Cell Biol., 107, 1995-2006

Keene, D.R. Maddox, B.K., Kuo, H.-J., Sakai, L.Y. and Glanville, R.W. 1991. Extractionof extendable beaded structures and their identification as fibrillin-containing extracellular matrix microfibrils. J. Histochem. Cytochem., 39, 441-449.

Speer, D.P. 1982. Collagenous architecture of the growth plate and perichondrial ossification groove. J. Bone Jt. Surg., 64-A, 399-407.

Figure legends

Figure 1. Schematic drawing of the distal femoral epiphyseal cartilage of adult *Rana catesbeiana*. The cartilage is inserted at the end of a tubular bone structure. The epiphyseal cartilage was divided into three main regions: articular cartilage (1), lateral articular cartilage (2) and growth cartilage (3). The short arrows point to the periosteal bone and the long arrow to the OCL. Bone marrow (bm). (Reprinted from Tissue & Cell, 31: 301-307. Felisbino & Carvalho, 1999, by permission of Churchill Livingstone.)

Figure 2. H&E stained longitudinal section of the epiphyseal cartilage of the bullfrog, showing the tip of the periosteal bone (pb), located between the growth cartilage (gc) and the lateral articular cartilage (lac). Attaching the lateral cartilage of the periosteal bone is the osteochondral ligament (ocl), which is composed of collagen fibers, cells and blood vessels (arrows), and is clearly composed of an innermost area (ia) and an outermost area (oa). X 100.

Figure 3. Toluidine blue stained cross section of the epiphyseal cartilage, showing some aspects of the osteochondral ligament. Osteoblasts (arrows) lined the surface of the periosteal bone (pb). Further from the bone surface there is a second layer of elongated and sinuous cells (arrowheads). The outer area of the OCL has fewer and dispersed cells and blood vessels (v). lac=lateral articular cartilage. X 200.

Figure 4. AlkPase activity was detected at the cell processes in the inner area of the OCL, while no reaction was observed in the outer area. Chondrocytes of the lateral cartilage also showed some AlkPase activity (arrows). pb= periosteal bone. X 250.

Figure 5. TRITC-phalloidin stained section of the bullfrog epiphyseal cartilage. Actin staining is concentrated in the inner area (ia) of the OCL. The periosteal bone (pb) and sites of ectopic calcification in the lateral cartilage (asterisks) were stained with calcein and appear green. Nuclei were stained with DAPI and appear blue. The arrow points to a blood vessel sectioned tangentially. X 250.

Figure 6. Higher magnification of the OCL after TRITC-phalloiding staining. Actin bundles are easily seen. A clear contrast in staining intensity is observed between cells of the inner area (ia) and those of the outer area (oa). X 500.

Figure 7. Immunocytochemistry for tubulin. Very weak staining was found. Tubulin is concentrated around the cell nucleus (arrows) in cells of both OCL areas. Tubulin is excluded from the processes of the cells in the inner area. The arrowhead points to a tangentially sectioned blood vessel. X 500.

Figure 8. Picrosirius-hematoxylin stained longitudinal section of the epiphyseal cartilage. Deeply stained thick collagen fibers formed fibrous insertions into the lateral cartilage (arrows). Thin and faintly stained collagen fibers run through the highly cellular area (ca) adjacent to the periosteal bone and insert (arrowheads) into the periosteal bone matrix (pb). X 400.

Figure 9. Same field as in figure 8 as viewed under the polarizing microscope. The collagen bundles inserted into the lateral articular cartilage (lac) show strong birefringence with orange to red interference colors (arrows). The thin fibers in the area adjacent to the bone show weaker birefringence with green to yellow interference colors. In this area the crossed arrangement of the collagen fibers, as well as their insertion into the bone matrix (arrowheads), is evident. X 400.

Figure 10. Longitudinal section of the epiphyseal cartilage, showing the immunoreactivity for type I collagen. Reaction was observed in the collagen fibers of the osteochondral ligament (ocl) and in the periosteal bone matrix (pb). X 200.

Figure 11. Longitudinal section of the epiphyseal cartilage, showing the immunoreactivity for type III collagen. Positive reaction was observed in the collagen bundles of the ligament (ocl) and in the outermost layer (arrows) of the periosteal bone (pb). X 200.

Figures 12 and 13. Longitudinal section of the epiphyseal cartilage, showing the immunoreactivity for type VI collagen. Positive reaction was observed on the surface of the collagen bundles in the osteochondral ligament (ocl). Figure 13 is an aspect of the distribution of type VI collagen, showing its concentration around a blood vessel (V) and on the surface of the collagen fibers (arrows). **12:** X 400; **13:** X 200.

Figure 14. Longitudinal section of the epiphyseal cartilage, showing the immunoreactivity for fibrilin 1. A positive reaction was found associated with the collagen bundles (arrows) of the osteochondral ligament (ocl). Periosteal bone (pb). X 400.

Figure 15. Picrosirius-hematoxylin stained longitudinal section of the epiphyseal cartilage. At the end of the lateral articular cartilage (lac), the collagen fibers of the osteochondral ligament (ocl) change their orientation and mix with the collagen fibers of the periosteum (po) of the periosteal bone (pb), which are longitudinally oriented and are continuous with the collagen fibers of the perichondrium (pe). The area showed in the micrograph is marked with a square on the scheme appearing in the inset. X 150.

Figure 16. Same field as in figure 15 as observed under polarized light, showing that the collagen fibers of the osteochondral ligament assume a longitudinal orientation on the periosteum. X 150.

Figure 17. TEM of the osteochondral ligament in the area of elongated cells. Cells were elongated and flat, with long and sinuous processes interspersed with the collagen fibrils. Their cytoplasm was rich in rough endoplasmic reticulum. It is evident that they are arranged parallel to each other and perpendicular to the bone surface. The area observed by TEM is marked in the light micrograph shown in the inset. ia=innermost area of the OCL. pb=periosteal bone; the arrowheads point to the osteoblasts on the bone surface. Inset: X 750; **17:** X 5,000.

Figure 18. TEM of the collagen fibrils in the area of the elongated cells. The cell processes are filled with microfilaments. The crossed distribution of the collagen fibrils is observed. X 33,000.

Figure 19. TEM of the osteochondral ligament at the insertion into the bone matrix. Collagen fibrils (col) of the osteochondral ligament extended into the mineralized matrix of the periosteal bone (pb). X 6,000.

Figure 20. TEM of the collagen fibrils in the outer area of the OCL close to the lateral cartilage. Collagen fibrils (col) are organized into thick and sinuous fibers. A fibroblast is observed in close association with an undulated collagen fiber. X 7,500.

Figure 21. TEM of a cell in the outer area of the OCL. The cell has an abundant cytoplasm filled with elements of the rough endoplasmic reticulum and secretory vesicles. X 16,000.

Figure 22. TEM of the extracellular matrix in the outer area of the OCL. Extracellular matrix microfibrils (arrows) were observed around the cells (asterisk) and amongst the collagen fibrils. X33,000.

Figure 23. TEM of a microfibril bundle (arrows), which was found on the surface of the collagen fibers in the outer area of the OCL. X33,000.

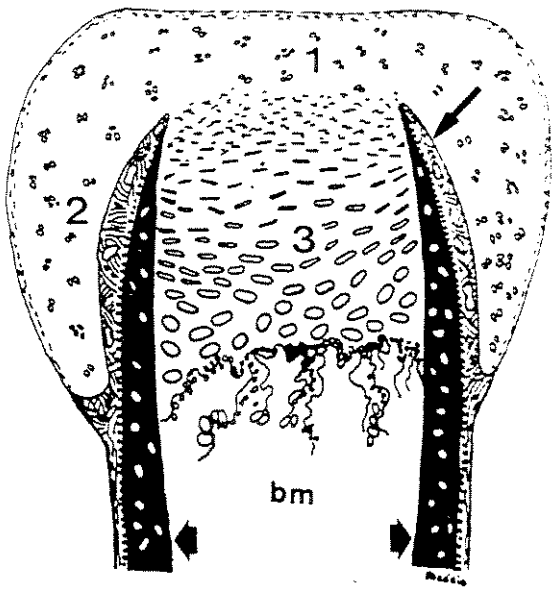

Figure 1.

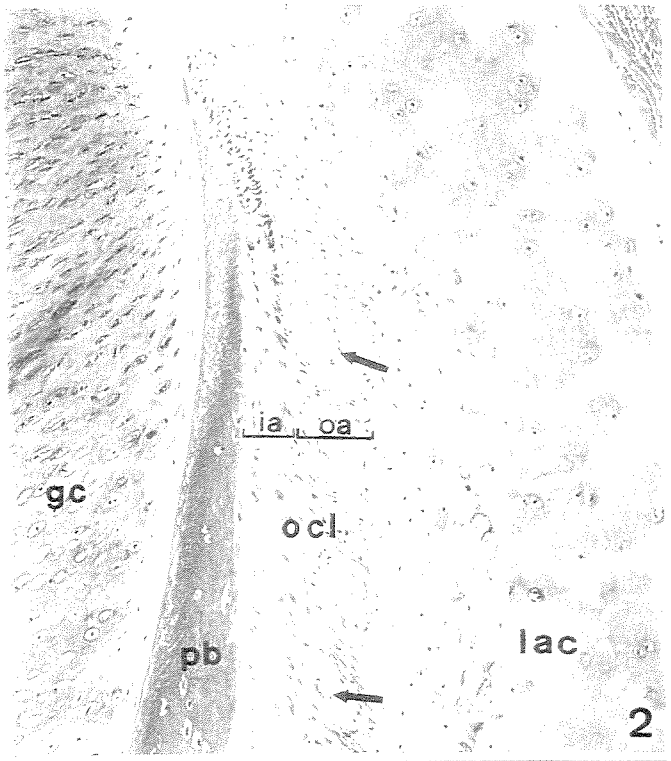
ia
oa
gc
ocl
pb
lac
2

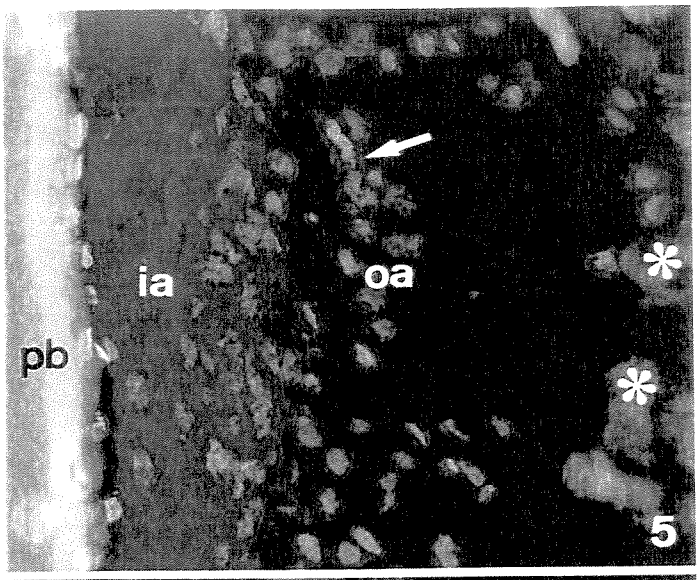
ia
oa
pb
5

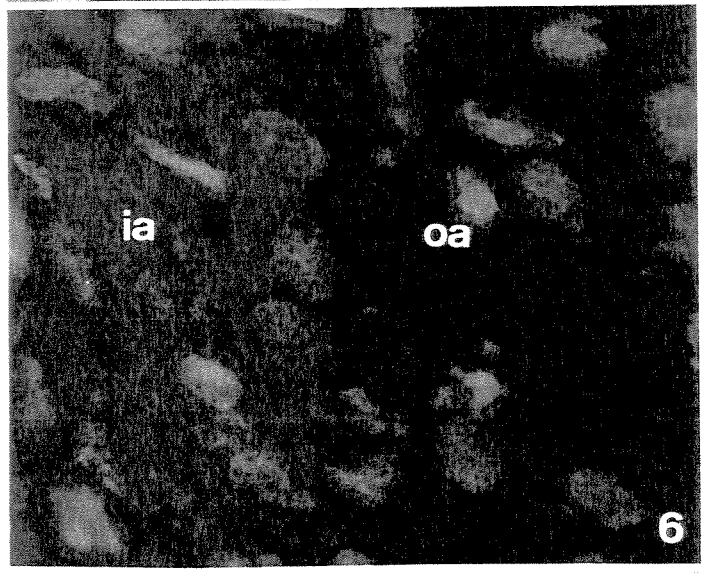
ia
oa
6

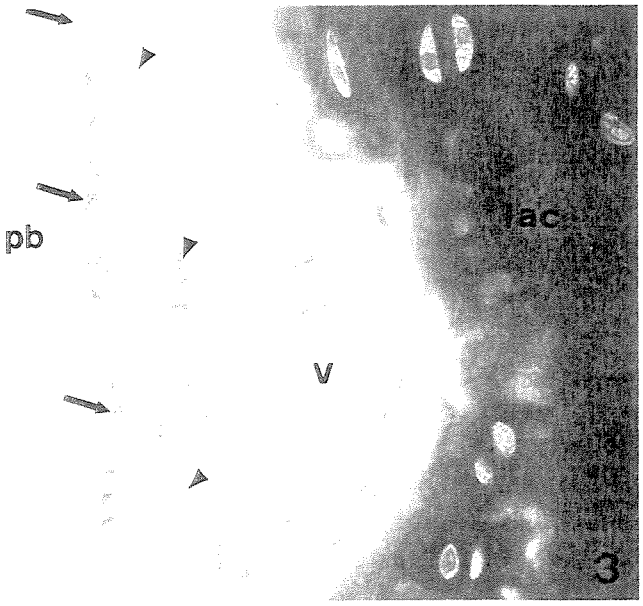
pb
lac
v
3

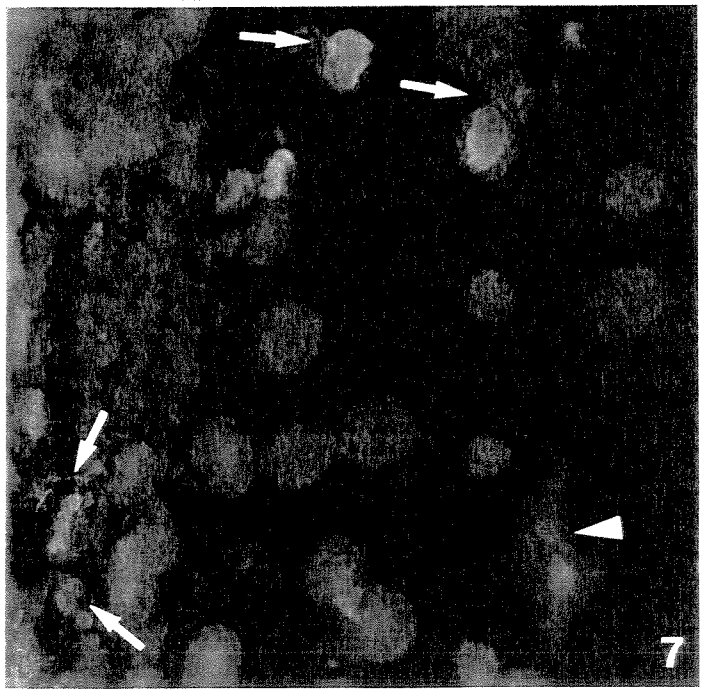
7

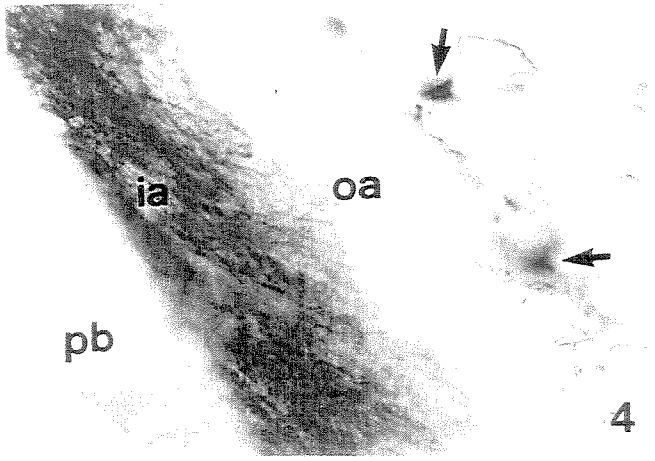
ia
oa
pb
4

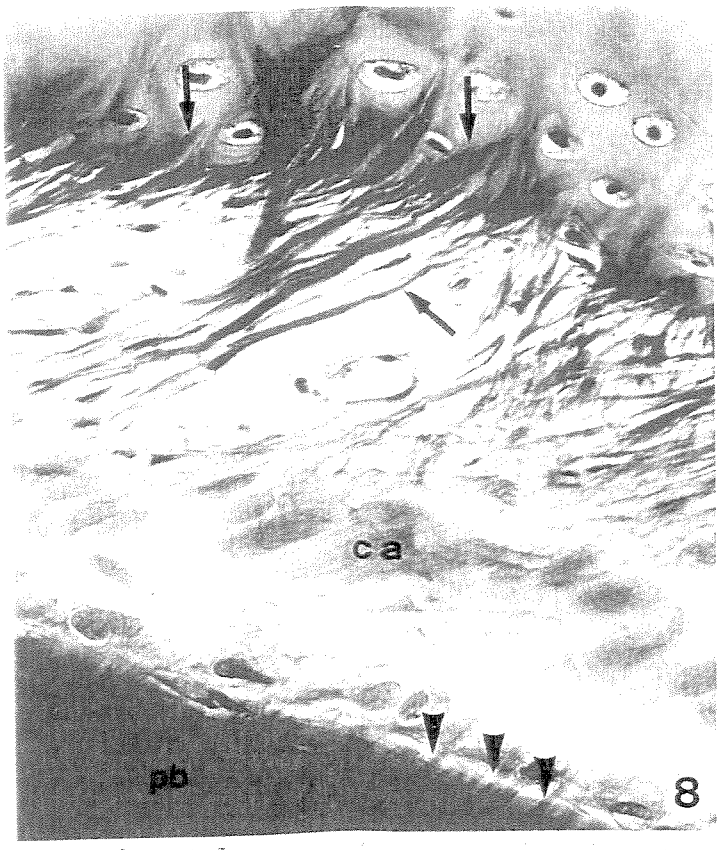
ca
pb
8


lac
9

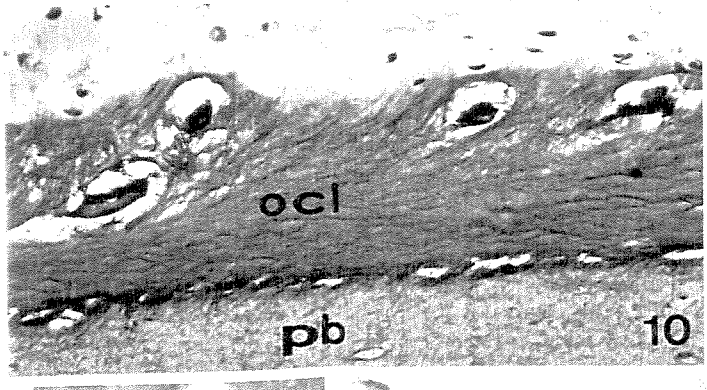
ocl
pb
10

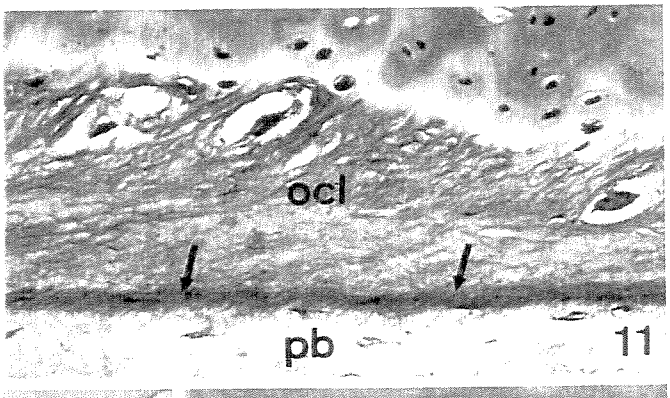
ocl
pb
11

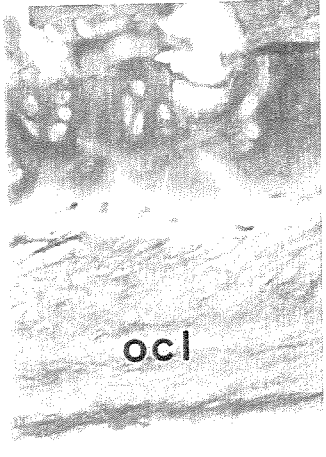
ocl
pb
12

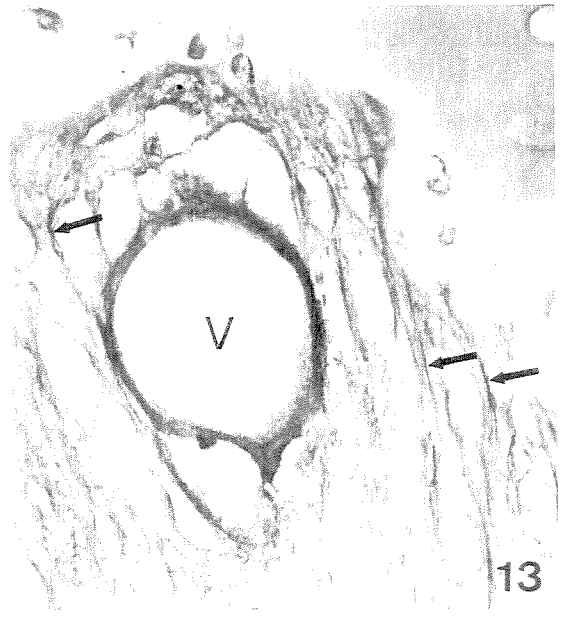
V
13

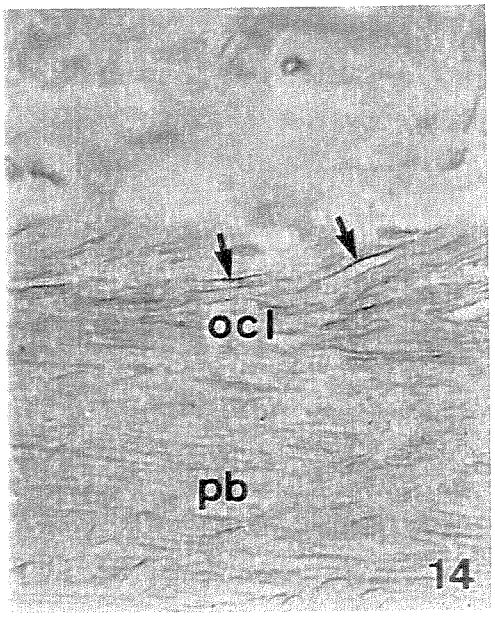
ocl
pb
14

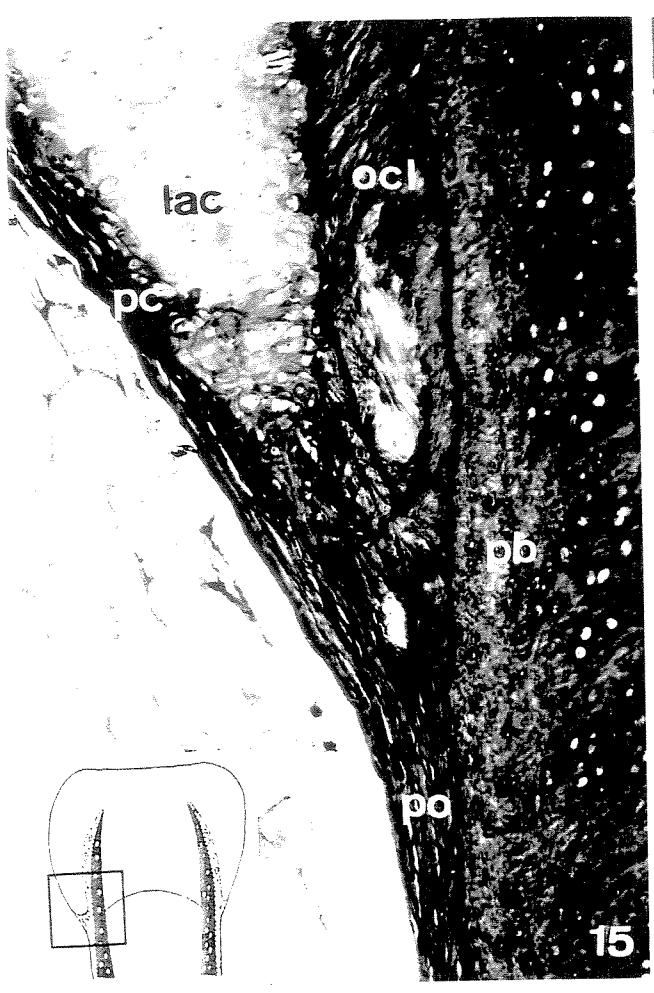
lac
ocl
pc
ob
po
15


16


oa
ia
17


18

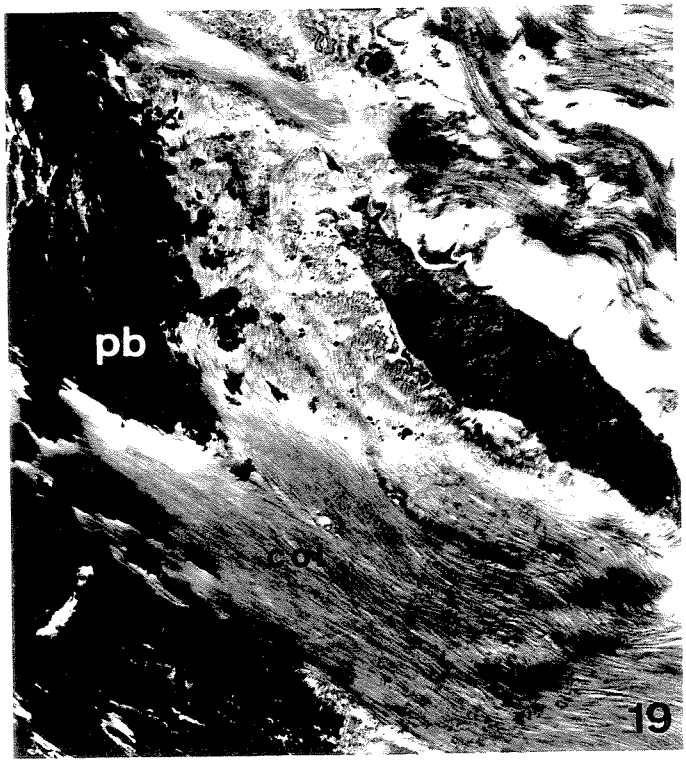
pb
col
19

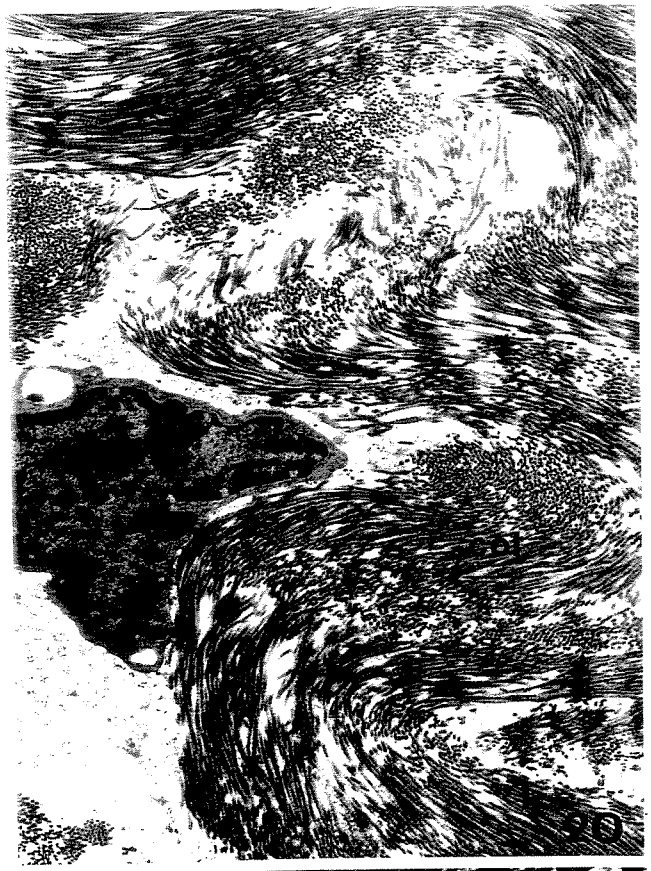

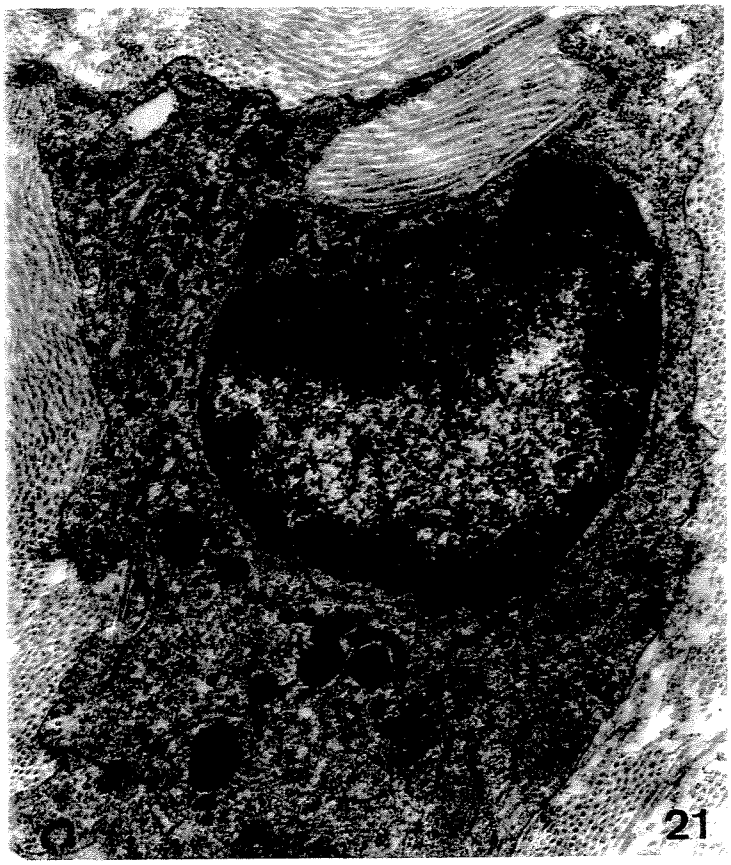

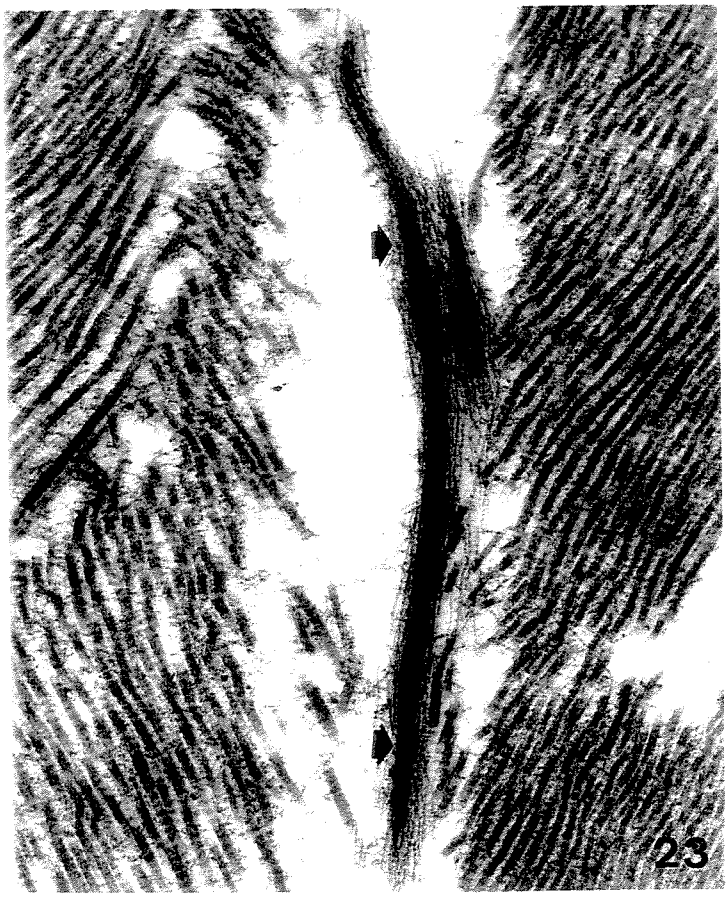

3.2. Growth cartilage calcification and the endochondral ossification in *Rana catesbeiana*. Submetido para publicação na revista Cell and Tissue Research

Abstract

Endochondral ossification in the growth cartilage of the long bones from the bullfrog *Rana catesbeiana* was examined. At 46-stage tadpole and 1-year-old animals, the hypertrophic cartilage had smooth contact with the bone marrow and the matrix did not contain any aspects of calcification or endochondral bone formation. However, in 2-year-old animals, matrix calcification and endochondral ossification were found. The matrix calcification appeared as isolated or coalesced spherical structures in the extracellular matrix of hypertrophic cartilage. Bone trabecular deposition was restricted to the central area of the hypertrophic cartilage surface exposed to the bone marrow. Cartilage matrix calcification and bone trabecular deposition were independent processes, since they were observed regardless of the presence of the other and calcified cartilage can be totally resorbed by multinucleated cells. Alkaline phosphatase activity was found at the plasma membrane of the chondrocytes from the lower proliferative zone to the lower hypertrophic chondrocyte in every animal used in this work, regardless of age. Osteoclasts were identified and were involved in calcified matrix resorption. DNA fragmentation as detected by the TUNEL reaction was found in all ages studied and was restricted to the lower hypertrophic zone. These results demonstrated that the endochondral ossification in *Rana catesbeiana* is a late event without contribution to the development and growth of the long bones, but with a possible role in the reinforcement of the bony structures as the animals gain weight in adulthood. They also showed that the deposition of bone trabeculae is not dependent on cartilage matrix calcification.

Introduction

Development and growth of bones via a cartilage model involves two distinct processes of ossification: perichondral or periosteal ossification and endochondral ossification. The first is the process whereby bone is formed outside, and around, cartilage and leads to the formation of a bone cortex. During bone growth, periosteal ossification continues at the leading edge of the growing bone cortex, around the upper zone of cartilage hypertrophy (Gardner and Gray, 1970; Osdoby and Caplan, 1981).

For the outher hand, endochondral ossification is a complex process in which the growth cartilage, inside the periosteal bone cortex, is progressively replaced by bony tissue. Cellular events, such as cell proliferation and hypertrophy, and matrix calcification are involved in this process. Furthermore, blood vessel invasion ocurrs bringing along with it osteoprogenitor cells, which then replace the calcified cartilage matrix with bone (Cancedda et al. 1995; Erlenbacher et al., 1995; Bianco et al. 1998).

The avian and mammalian process of endochondral ossification is well established. Calcification of the longitudinal septae is important to direct the chondrocyte hypertrophy into longitudinal expansion of the growth cartilage. Then, the calcified matrix is used as a scaffold for the deposition of bone trabeculae by the osteoblasts (Hunziker 1994). Alkaline phosphatase (AlkPase) activity at the plasma membrane of the hypertrophic chondrocytes and matrix vesicle production are assumed to be essential for matrix calcification (Leboy et al 1989; Anderson 1995; Kirsch et al. 1997). Programmed cell death of the hypertrophic chondrocyte is also a characteristic aspect of the growth plate. Some authors believe that apoptosis is the only fate of the hypertrophic chondrocytes (Kim 1995; Zenmyo et al. 1996; Gibson 1998), but others suggest that these cells may dedifferentiate to osteoblast-like cells and take part in bone formation (Gentili et al. 1993, Roach et al. 1995; Gerstenfeld and Shapiro 1996; Roach 1997; Bianco et al. 1998). Another characteristic of the avian and mammalian growth plates is the expression of type X collagen (Schimid and Conrad 1982; Schimid and Linsenmayer 1983; Gibson and Flint 1985; Sandell et al. 1994). Type X collagen expression takes place in the hypertrophic zone and its function is probably to prepare the matrix for blood vessel invasion and/or calcification (Kwan et al. 1991; Bruckner and van der Rest 1994; Olsen 1995). However, its involvement in the whole process is questionable, since the null mice for type X collagen showed normal long bone growth and development (Rosati et al. 1994).

None of these aspects related to the physiology of the bone growth is known for the amphibian growth cartilage.

Anurans are in a lower phylogenetic position as compared to birds and mammals. Furthermore, anurans present very distinct movement and posture behavior, which obviously affect the structure, composition and organization of the extracellular matrix of tendons (Carvalho and Vidal 1994, Carvalho 1995; Carvalho and Felisbino 1999), bones and cartilages (Haines 1942; Dickson 1982; Dell'Orbo et al 1992; Felisbino and Carvalho 1999).

In a previous study we described the structure of the epiphyseal cartilage of *R. catesbeiana* (Felisbino and Carvalho, 1999). The epiphyseal cartilage is plugged into the end of a tubular bone shaft, defining three regions: articular cartilage, lateral articular cartilage and growth cartilage. The growth cartilage is inside the bone tube. In the proliferative zone there is a perpendicular separation of daughter cells and no columnar arrangement of the chondrocytes is observed. Neither hypertrophic matrix calcification nor endochondral ossification were found in the 1-year-old animals and these aspects led us to conclude that long bone extension depends mostly on periosteal ossification. A 200μm long fibrous region at the extremity of the periosteal bone tube is continuously produced by osteoblasts and subsequently mineralized (Felisbino and Carvalho, 2000). This region has a counterpart in the mammalians and birds, which is located at the Ranvier groove (Shapiro et al. 1977). However, it is much more prominent in the bullfrog.

Based on this previous report we decided to investigate whether endochondral ossification and other events related to this process took place in the bullfrog cartilage, with special attention to matrix calcification, bone trabecular deposition, alkaline phosphatase activity and chondrocyte death, in comparison with the current models for the avian and mammalian growth plate. The results presented here suggest that endochondral ossification does not play an essential role in long bone development and growth in this anuran, it being a late event, probably involved with the reinforcement of the bone ends, as the animals gain weight in adulthood.

Materials and Methods

Animals

Specimens of *R. catesbeiana* were obtained from a farm in Atibaia (São Paulo State, Brazil) where they were fed with an artificial diet *ad libitum*. They were divided into tree age groups. The first group consisted of tadpoles at 46-stage of larval development (transformation completed), which were about 6 months old (Gosner 1960). The second group had young 1-year-old animals (about six months post-transformation) and the third one consisted of 2-year-old animals (18 months post-transformation).

Animals in the first group weighed about 10g and measured ~40mm (snout to urostyle). The second and third groups showed a mean weight of 120g and 230g, respectively and measured 90mm and 130mm, respectively. These measures indicates that the frogs reared for the food market grow much faster than those in the wild, since the values for the second and third groups

correponded to 3 and 5-year-old animals monitored in the nature, respectively (Shirose et al. 1993). In their studies, Shirose et al. collected animals that lived up to nine years.

The animals were killed by decapitation after cold immobilization and the distal femoral (DF) epiphyseal cartilages dissected out and immediately fixed by immersion as described below.

Histochemistry

Cartilage fragments were fixed in 4% formaldehyde in phosphate buffer at pH7.4, containing 0.85% NaCl (PBS) for 24 hours. Some samples were decalcified in 4% formaldehyde, 10% acetic acid and 0.85% NaCl solution for 15 days. The material was then dehydrated in a graded ethanol series, clarified in Cedar wood oil and embedded in Paraplast Plus embedding medium. Some fragments were embedded in Polysciences JB4 resin. Serial sagittal Paraplast (6μm) sections or resin (2μm) sections were stained by, hematoxylin-eosin (HE), toluidine Blue (TB), picrosirius-hematoxylin (PSH) (Junqueira et al. 1979) or subjected to the von Kossa's reaction for calcified matrix.

Enzyme histochemistry

Some tissue fragments were fixed in 4% formaldehyde in 0.1M cacodylate buffer at pH 7.2 for 4 hours, washed with the same buffer, treated with 70% ethanol and embedded in JB4 historesin. Two-micrometer thick sections were assayed for alkaline phosphatase (AlkPase) activity using 0.1% α-naphtyl phosphate, 0.1% fast red and 50mM $MgCl_2$ in 0.1M tris-malate buffer at pH10. For the identification of osteoclasts, the same compounds were used in 0.1M acetate buffer at pH5.0 plus 50mM sodium tartrate for tartrate-resistant acid phosphatase (TRAP) activity. The controls were prepared using the same solutions without α-naphtyl phosphate (Bancroft 1982; Cole and Wezeman 1987). Sections were counter-stained with methyl-green.

DNA fragmentation

DNA fragmentation was detected by *in situ* labeling with the terminal deoxynucleotidyl transferase (TdT-FragEl - Oncogene Research Products). Paraplast sections were treated with proteinase K and 3'-end labeled with fluorescein-conjugated dUTP. An incubation step with a peroxidase-conjugated rabbit anti-fluorescein antibody was followed by the DAB reaction.

Sections were counter-stained with methyl green. Negative controls were processed without the enzyme.

Transmission electron microscopy (TEM)

Fragments of the growth cartilage from 1 and 2-year-old animals were processed for TEM. Tissue fragments ($1mm^3$) were fixed with 3% glutaraldehyde plus 0.25% tannic acid in Millonig's buffer containing 0.54% glucose (Cotta-Pereira et al. 1976). Tannic acid was chosen for a better preservation and visualization of the fibrillar components. After washing with the same buffer, the material was post-fixed with 1% osmium tetroxyde, washed again, dehydrated in graded acetone, and embedded in Epon 812. Ultrathin silver sections were cut using a diamond knife on a LKB ultramicrotome and contrasted with alcoholic uranyl acetate and lead citrate. Grids were examined in a Leo 906 transmission electron microscope operating at 80 kV.

Results

The DF epiphyseal cartilages of *R. catesbeiana* are attached to the extremity of the periosteal bone shaft and are formed of a voluminous hyaline cartilage, which shows three main regions: the articular cartilage, the lateral articular cartilage and the growth cartilage. The growth cartilage is inside the periosteal bone (Fig. 1) and, since there is no secondary center of ossification, isolating the growth cartilage (as a disc or a plate) from the articular cartilage, the term growth plate does not apply (Felisbino and Carvalho, 1999).

The hypertrophic zone of the epiphyseal cartilage in 46-stage tadpole (Fig. 2) and in 1-year-old bullfrogs (Fig. 3) showed a regular contact with the bone marrow. Neither cartilage calcification or endochondral bone was observed in any of the individuals of these two groups.

Endochondral bone and matrix calcification was found in the DF growth cartilage of 2-year-old animals (Fig. 4). In these animals, the hypertrophic cartilage showed an irregular contact with the bone marrow, in contrast to the younger ones. At the transition of the cartilage with the bone marrow, bone trabeculae were identified by intense staining with PSH (and the characteristic birefringence at the polarizing microscope) (Fig.4), and by the positive response to the von Kossa's reaction (not showed).

A positive response to the von Kossa's reaction was also identified in the maturation zone. The reactive structures were small dots, which became progressively larger towards the hypertrophic zone (Figs. 5 and 6). The hypertrophic cartilage of some 2-year-old animals,

contained matrix calcification, but no endochondral bone (Fig. 5). Calcification sites were observed as single or coalesced spherical structures in the decalcified cartilage and showed more intense staining with PSH (Fig. 7). Furthermore, calcified matrix not associated with endochondral bone was found inside bone marrow sunrounded by multinucleated cells (Fig 8). In some others, endochondral bone formation was found in association with uncalcified cartilage matrix (Figs. 9 and 10). These variable aspects were confirmed by inspection of serial sections of the cartilage full thickness and showed no evident relationship with sex, size or any anatomic variation.

AlkPase activity was associated with the plasma membrane of the hypertrophic chondrocytes in all ages (Figs. 11-13) and also in the extracellular matrix of the hypertrophic zone of 1-year-old animals (Fig. 12). The AlkPase activity first appears in the plasma membrane of the chondrocytes in the lower proliferative zone (Fig. 14). AlkPase activity was also found in the osteoblasts in contact with the bone trabeculae in the 2-year-old animals (Fig. 14).

Multinucleated cells with polarized cytoplasm and positive TRAP reactions were detected on the surface of either bone trabeculae or calcified cartilage in the 2-year-old animals (Fig. 16).

DNA fragmentation was found in cells of the lower hypertrophic cartilage in animals from the different age groups (Figs. 17-20). These apoptotic chondrocytes were only found in a short distance, about three cell layer, of the transition to the bone marrow.

TEM analysis of one-year-old animal growth cartilage showed mononucleated cells in contact with non-calcified cartilage matrix in the transition of the hypertrofic zone with bone marrow (Fig 21). In the two-year-old animal growth cartilage, many matrix vesicles were found in the extracellular matrix of the upper hypertrophic zone (Fig. 22). In the lower hypertrophic zone of two-year-old animal growth cartilage, spherical structure of calcified cartilage matrix, isolated or coalesced were found (Fig. 23). This spherical structures of calcified matrix were found inside bone marrow sunrounded by binucleated cells with evident nucleolus and many vesicles in the cytoplasm (Fig 24).

We also examined the proximal femoral and tibio-fibula growth cartilages and the results presented here for the distal femoral growth cartilage are representative for all of them, except that in the proximal tibio-fibula, bone trabeculae were difficult to find.

The results are summarized in Table 1.

Discussion

Though the role of the growth cartilage and endochondral ossification in long bone growth is well defined for avians and mammals (Hunziker and Schenk 1989, Breur et al. 1991, 1992; Barreto et al. 1993, Farnum and Wilsman 1993, Wilsman et al. 1996), its function in anurans is poorly understood (Dickson 1982, Dell'Orbo et al. 1992), mainly because the anuran growth cartilage presents distinctive aspects when compared to the mammalian and avian models.

In this study, we examined the endochondral ossification in *R. catesbeiana* and demonstrated that it is a delayed process. Bone trabeculae originated from endochondral ossification were not found in these animals until 2-year-old. It means that periosteal ossification until 2-year-old is not followed, internaly, by cartilage calcification and bone trabeculae deposition. The uncalcified cartilage is resorbed just for the formation of the bone marrow cavity. This fact is consistent with the idea that long bone development and growth up to adulthood depend mostly on periosteal ossification (Dickson 1982; Dell'Orbo et al. 1992; Felisbino and Carvalho, 1999). Furthermore, some aspects of endochondral ossification in bullfrog growth cartilage differ from the observed in the avian and mammalian models.

Cartilage calcification, when present (in 2-year-old animals), is not a necessary factor for the formation of bone trabeculae, since osteoblasts may deposit bone on the surface of the uncalcified cartilage. The calcified cartilage may be totally resorbed by osteoclasts or be used as a anlage for the deposition of bone trabeculae. These aspects of the endochondral ossification in the bullfrog may represent an economic adaptation for bone growth process or an uncompleted regulated process.

Cartilage calcification also showed unique aspects in the bullfrog cartilage, appearing as isolated or coalesced spherical structures. Spherical scaffolds were recently described for the calcified cartilage in the thyroid (Kimpel et al. 1998), but were not described during calcification of the growth cartilage. Dickson (1982) and Dell'Orbo et al. (1992) did not report on the presence of these structures for *R. temporaria* and *R. esculenta*, respectively.

AlkPase activity is always associated with calcification and it is thought to be responsible for the production of inorganic phosphate (Anderson, 1995). However, in the bullfrog growth cartilage, AlkPase activity appeared at the plasma membrane of chondrocytes much earlier than calcification. This activity seems to be a constitutive characteristic of the chondrocyte differentiation in the bullfrog growth cartilage and other factors must be necessary for

endochondral ossification takes place. This observation are consistent with the hypothesis that mechanical loanding constitute an important influence during skeletal morphogenis (Carter and Wong, 1988; van't Veen et al. 1995)

Besides describing aspects of the growth cartilage physiology in the bullfrog, this paper demonstrates that chondrocyte hypertrophy and death, as well as matrix calcification are neither directly associated to each other nor to the formation of endochondral bone.

Since these events are spatially and timely associated in the mammalian and avian systems, the bullfrog seems to represent a valuable model for the study of chondrocyte differentiation and endochondral ossification.

References

Anderson HC (1995) Molecular biology of matrix vesicles. Clin Orthop 34: 266-280

Arsenault AL, Kohler DM (1994) Image analysis of the extracellular matrix. Microsc Res Tech 28: 409-421

Bancroft JD (1982) Enzyme histochemistry. In: Bancroft JD, Stevens A (eds) Theory and Practice of Histological Techniques. Churchill Livingstone. Edinburgh pp 384-387

Barreto C, Albrecht RM, Bjorling DE, Horner JR, Wilsman NJ (1993) Evidence of the growth plate and the growth of long bones in juvenile dinosaurs. Science 262: 2020-2023

Bianco P, Cancedda FD, Riminucci M, Cancedda R (1998) Bone formation via Cartilage Models: The "borderline chondrocytes". Matrix Biol 17: 185-192

Breur GJ, vanEnkevort BA, Farnum CE, Wilsman NJ (1991) Linear relationship between the volume of hypertrophic chondrocytes and the rate of longitudinal bone growth in growth plates. J Orthop Res 9: 348-359

Breur GJ, Farnum CE, Padgett GA, Wilsman NJ (1992) Cellular basis of decreased rate of longitudinal growth of bone in pseudoachondroplastic dogs. J Bone Joint Surg 74-A: 516-528

Bronckers ALJJ, Goei W, van Heerde WL, Dumont EAWJ, Reutelingsperger CPM, van den Eijnde SM (2000) Phagocytosis of dying chondrocytes by osteoclasts in the mouse growth plate as demonstrated by annexin-V labelling. Cell Tissue Res 301: 267-272

Bruckner P, van der Rest M (1994) Structure and function of cartilage collagens. Microsc Res Tech 28: 378-384

Cancedda R, Cancedda FD, Castagnola P (1995) Chondrocyte differentiation. Int Rev Cytol 159: 265-359

Carter DR, Wong M (1988) The role of mechanical loading histories in the developmet of diarthrodial joints. J Orthop Res 6: 804-816

Carvalho H.F, Vidal BC (1994) The unique fibrillar arrangement of the bullfrog pressure-bearing tendon as an indicative of great functional deformability. Biol Cell 82: 59-65

Carvalho H.F (1995) Understanding the biomechanics of tendon fibrocartilages. J Theor Biol 172: 293-297

Carvalho HF, Felisbino SL, (1999) The development of the pressure-bearing tendon in the bullfrog *Rana catesbeiana.* Anat Embryol 200: 55-64

Cole AA, Wezeman FH (1985) Perivascular cells in cartilage canals of the developing mouse epiphysis. Am J Anat 174: 119-129

Cole AA, Wezeman FH (1987) Cytochemical localization of tartrate-resistant acid phosphatase, alkaline phosphatase, and nonspecific esterase in perivascular cells of cartilage canals in the developing mouse epiphysis. Am J Anat 180: 237-242

Dell'Orbo C, Gioglio L, Quacci D (1992) Morphology of epiphyseal apparatus of a ranid frog. Histol Histopathol 7: 267-273

Dikson RG (1982) Ultrastructure of growth cartilage in the proximal femur of the frog, *Rana temporaria*. J Anat 135: 549-564

Elerbacher A, Filvaroff EH, Giltelman SE and Derynck R (1995) Toward a molecular understanding of skeletal development. Cell 80: 371-378

Farnum CE, Wilsman NJ (1993) Determination of proliferative characteristics of growth plate chondrocytes by labeling with bromodeoxyuridine. Calcif Tissue Int 52: 110-119

Felisbino SL, Carvalho HF (1999) The epiphyseal cartilage and growth of long bones in *Rana catesbeiana*. Tissue Cell 31: 301-307

Felisbino SL, Carvalho HF (2000) The osteochondral ligament: a fibrous attachment between bone and articular cartilage in *Rana catesbeiana*. Tissue Cell 32: 527-536.

Gallo RL, Dorschner RA, Takashima S, Klagsbrun M, Eriksson E, Bernfield M (1997) Endothelial cell surface alkaline phosphatase activity is induced by IL-6 released during wound repair. J Invest Dermatol 109: 597-603

calcification to take place besides this enzyme activity. The production of matrix vesicles as initiators of calcification has been assumed to be a finely controlled mechanism for matrix calcification (Anderson 1995; Kirsch et al. 1997; Roach 1999). The presence of AlkPase activity in the extracellular matrix of the 1-year-old hypertrophic cartilage may represent an initial step in the calcification observed in the 2-year-old animals. And the location of the extracellular AlkPase activity corresponds to that of matrix vesicles (unpublished results).

It has been proposed that matrix vesicles are chondrocyte's apoptotic bodies (Kim 1995; Hashimoto et al. 1998). This is in agreement with the hypothesis that terminally differentiated chondrocytes die by apoptosis (Hatori et al. 1995; Gibson et al. 1997). However, matrix vesicles are also found in the proliferation and maturation zones, where apoptosis has not been detected (Poole 1991; Arsenault and Kohler 1994; Wu et al. 1997). So, the relationship between matrix vesicle production and chondrocyte apoptosis remains controversial. We have found that hypertrophic chondrocytes die by apoptosis, as shown by DNA fragmentation and morphological aspects. Since it was detected in all animals irrespective of age, and matrix calcification takes place mainly in the 2-year-old animals, we may conclude that there is no direct relationship between the two events, at least in *R. catesbeiana*. As no empty intact lacunae were found in the lower hypertrophic cartilage, we believe that apoptotic chondrocytes are released into the bone marrow and/or phagocytosed by mononucleated cells, probably macrophages, or even by osteoclasts as suggested by Bronckers and coworkers (2000) for other especies.

While mononucleated cells are responsible for the resorption of the uncalcified cartilage in young animals, the detection of TRAP activity (Minkin 1982), allowed the identification of osteoclasts in contact with calcified cartilage and/or bone trabeculae in 2-year-old animals. These two aspects, the resorption of calcified cartilage and bone by osteoclasts and the resorption of uncalcified cartilage by mononucleated cells, are similar to those taking place in birds and mammals (Schenk et al. 1967; Cole and Wezeman 1985; 1987). However, we found osteclasts associated with isolated calcified cartilage spheres inside the bone marrow. Problably, the resorption of the uncalcified cartilage matrix by monucleated cells release such calcified cartilage into the bone marrow.

In conclusion, endochondral ossification is a late event and does not play an essential role in the development and growth of long bones in *R. catesbeiana*. However, as the animals grow older and gain weight, further reinforcement of the bone ends is apparently necessary and

Gardner E, Gray DJ (1970) The prenatal development of the human femur. Am J Anat 129: 121-140

Gentili C, Bianco P, Neri M, Malpeli M, Campanile G, Castagnola P, Cancedda R, Cancedda FD (1993) Cell proliferation, extracellular matrix mineralization, and ovotransferrin transient expression during in vitro differentiation of chick hypertrophic chondrocytes into osteoblast-like cells. J Cell Biol 122: 703-712

Gerstenfeld LC, Shapiro FD (1996) Expression of bone-specific genes by hypertrophic chondrocytes: Implications of the complex functions of the hypertrophic chondrocyte during endochondral bone development. J Cell Biochem 62: 1-9

Gibson G (1998) Active role of chondrocyte apoptosis in endochondral ossification. Microsc Res Tech 43: 191-204

Gibson GJ, Flint MH (1985) Type X collagen synthesis by chick sternal cartilage and its relationship to endochondral development. J Cell Biol 101: 277-284

Gibson G, Lin DL, Roque M (1997) Apoptosis of terminally differentiated chondrocytes in culture. Exp Cell Res 233: 372-382

Gosner KL (1960) A simplified table for staging Anura embryos and larvae with notes on identification. Herpetol 16: 183-190

Haines RW (1942) The evolution of epiphyses and of endochondral bone. Biol Rev 17: 267-292

Hashimoto S, Ochs RL, Rosen F, Quach J, McCabe G, Solan J, Seegmiller JE, Terkeltaub R, Lotz M (1998) Chondrocyte-derived apoptotic bodies and calcification of articular cartilage. Proc Natl Acad Sci USA. 95: 3094-3099

Hatori M, Klatte KJ, Teixeira CC, Shapiro IM (1995) End labeling studies of fragmented DNA in the avian growth plate: Evidence of apoptosis in terminally differentiated chondrocytes. J Bone Miner Res. 10: 1960-1968

Hunziker EB, Schenk RK (1989) Physiological mechanisms adopted by chondrocytes in regulating longitudinal bone growth in rats. J Physiol 414: 55-71

Hunziker EB (1994) Mechanism of longitudinal bone growth and its regulation by growth plate chondrocytes. Microsc Res Tech 28: 505-519

Junqueira LC, Bignolas G, Brentani RR (1979) Picrosirius staining plus polarization microscopy, a specific method for collagen detection in tissue sections. Histochem J 11: 447-455

Kim KM (1995) Apoptosis and calcification. Scanning Microsc 9: 1137-1178

Kimpel M, Claassen H, Fleiner B, Tillmann B (1999) Vascularization and cartilage mineralization of the thyroid cartilage of Munich minipigs and domestic pigs. Anat Embryol 199: 281-290

Kirsch R, Nah HD, Shapiro IM, Pacifici M (1997) Regulated production of mineralization-competent matrix vesicles in hypertrophic chondrocytes. J Cell Biol 137: 1149-1160

Kwan API, Cummings CE, Chapman JA, Grant ME (1991) Macromolecular organization of chicken type X collagen in vitro. J Cell Biol 114: 597-604

Leboy PS, Vaias L, Uschmann B, Golub E, Adams SL, Pacifici M (1989) Ascorbic acid induces alkaline phosphatase, type X collagen, and calcium deposition in cultured chick chondrocytes. J Biol Chem 264: 17281-17286

Minkin C (1982) Bone acid phosphatase: Tartrate-resistant acid phosphatase as marker of osteoclast function. Calcif Tissue Int 34: 285-290

Olsen BR (1995) Mutations in collagen genes resulting in metaphyseal and epiphyseal dysplasias. Bone 17: 45S-49S

Osdoby P, Caplan AI (1981) First bone formation in the developing chick limb. Develop Biol 86: 147-156

Poole AR (1991) The growth plate: Cellular physiology, cartilage assembly and mineralization. In: Hall BK, Newman SA (eds) Cartilage: Molecular aspects. CRC Press, Boca Raton, FL, pp 179-211

Roach HI, Erenpreisa J, Aigner T (1995) Osteogenic differentiation of hypertrophic chondrocytes involves asymmetric cell divisions and apoptosis. J Cell Biol 131: 483-493

Roach HI (1997) New aspects of endochondral ossification in the chick: chondrocyte apoptosis, bone formation by former chondrocytes, and acid phosphatase activity in the endochondral bone matrix. J Bone Miner Res 12: 795-805

Roach HI (1999) Association of matrix acid and alkaline phosphatase with mineralization of cartilage and endochondral bone. Histochem J 31: 53-61

Rosati R, Horan GSB, Pinero GJ, Garofalo S, Keene DR, Horton WA, Vuorio E, de Crombrugghe B, Behringer RR (1994) Normal long bone growth and development in type X collagen-null mice. Nature Genet 8: 129-135

Sandell LJ, Sugai JV, Trippel SB (1994) Expression of collagens I, II, X, and XI and Aggrecan mRNAs by bovine growth plate chondrocytes *in situ*. J Orthop Res 12: 1-14

Schenk RK, Spiro D, Wiener J (1967) Cartilage resorption in the tibial epiphyseal plate of growing rats. J Cell Biol 34: 275-291

Schmid TM, Conrad HE (1982) A unique low molecular weight collagen secreted by cultured chick embryo chondrocytes. J Biol Chem 25: 12444-12450

Schmid TM, Linsenmayer TF (1983) Short chain (pro)collagen from aged endochondral chondrocytes. Biochemical characterization. J Biol Chem 258: 9504-9509

Shapiro F, Holtrop ME, Glimcher MJ (1977) Organization and cellular biology of the perichondrial ossification groove of Ranvier. J Bone Joint Surg 59A: 703-723

Schultz-Hector S, Balz K, Bohm M, Ikehara Y, Rieke L (1993) Cellular localization of endothelial alkaline phosphatase reaction product and enzyme protein in the myocardium. J Histochem Cytochem 41: 1813- 1821

Shirose LJ, Brooks RJ, Barta JR, Desser SS (1993) Intersexual differences in growth, mortality, and size at maturity in bullfrogs in central Ontario. Can J Zool 71: 2363-2369

Van't Veen SJGA, Hagen JW, Van Ginkel FC, Prahl-Andersen B, Burger EH (1995) Intermittent compression stimulates cartilage mineralization. Bone 17: 461-465

Wilsman NJ, Farnum CE, Lieferman EM, Fry M, Barreto C (1996) Differential growth by growth plates as a function of multiple parameters of chondrocytic kinetics. J Orthop Res 14: 927-936

Wu LN, Wuthier MG, Genge BR, Wuthier RE (1997) In situ levels of intracellular Ca2+ and pH in avian growth plate cartilage. Clin Orthop 335: 310-324

Zenmio M, Komiya S, Kawabata R, Sasaguri Y, Inoue A, Morimatsu M (1996) Morphological and biochemical evidence for apoptosis in the terminal hypertrophic chondrocytes of the growth plate. J Pathol 180: 430-433

Legends

Figure 1. Schematic drawing of the distal femoral epiphyseal cartilage of adult *Rana catesbeiana*. The cartilage is inserted at the end of a tubular bone structure. The epiphyseal cartilage can be divided into three main regions: articular cartilage (1), lateral articular cartilage (2) and growth cartilage (3). The short arrows point to the periosteal bone. Bone marrow (bm). (Reprinted from Tissue & Cell, 31: 301-307. Felisbino & Carvalho, 1999, by permission of Churchill Livingstone.)

Figure 2. 46-Stage tadpole. PSH-stained longitudinal section of the decalcified DF growth cartilage. The hypertrophic cartilage (hc) presented a smooth contact with the bone marrow (bm) and there was neither endochondral ossification nor matrix calcification. Note the absence of a columnar arrangement of the chondrocytes and the abundant extracellular matrix between them. Scale bar, 100μm.

Figure 3. One-year-old animal. PSH-stained longitudinal section of the decalcified DF growth cartilage. The hypertrophic cartilage (hc) presented a smooth contact with the bone marrow (bm) and there was neither endochondral ossification nor matrix calcification. Scale bar, 100μm.

Figure 4. Two-year-old animal. PSH-stained longitudinal section of the decalcified DF growth cartilage. The hypertrophic cartilage (hc) presented an irregular border with the bone marrow (bm). Strongly stained bone trabeculae were found on the border of the cartilage (arrows) and PSH-positive structures was observed in the extracellular matrix of the cartilage (arrowheads). Scale bar, 200μm.

Figure 5. Two-year-old animal. Longitudinal historesin section of the non-decalcified DF growth cartilage subjected to the von Kossa's reaction. The von Kossa's reaction demonstrated the presence of calcium deposits (black stained) in the extracellular matrix of the hypertrophic cartilage (hc). Note that there was no orientation of the calcification product and there were no bone trabeculae in the transition to the bone marrow (bm). Methyl green counter-staining. Scale bar,100μm.

Figure 6. Detail of figure 8 showing rounded (arrowheads) and coalesced (arrows) structures associated with calcification in the bullfrog cartilage. von Kossa's reaction plus methyl green counter-staining. Scale bar, 20μm.

Figure 7. Detail of figure 7 showing the isolated and coalesced spherical structures (arrowheads) associated with calcification of the extracellular matrix. Scale bar, 20μm.

Figure 8. Two-year-old animal. TB-stained longitudinal JB_4 resin section of non-decalcified DF growth cartilage. Calcified cartilage matrix not associated with endochondral bone (arrow) was found inside the bone marrow sunrounded by multinucleated cells (arrowheads) with evident nucleoli. Scale bar, 20μm.

Figure 9. Two-year-old animal.. A positive reaction to von Kossa's in the bone trabecula (arrow) localized on the border of the hypertrophic cartilage (hc) with the bone marrow (bm). Note that there was no calcification of the extracellular matrix of the hypertrophic cartilage. Methyl green counter-staining. Scale bar, 100μm.

Figure 10. Same field as figure 8 as observed under polarized light. The bone trabecula exhibited the typical birefringence of collagenous structures (arrow). Scale bar, 100μm.

Figure 11. 46-Stage tadpole. Longitudinal historesin section of the non-decalcified DF growth cartilage. Alkaline phosphatase activity was detected at the plasma membrane of the hypertrophic chondrocytes (arrows). Methyl green counter-staining. Scale bar, 20μm.

Figure 12. One-year-old animal. Longitudinal historesin section of the non-decalcified DF growth cartilage. Alkaline phosphatase activity was detected at the plasma membrane of the hypertrophic chondrocytes (arrows) and in the extracellular matrix (arrowheads). Methyl green counter-staining. Scale bar, 20μm.

Figure 13. Two-year-old animal. Longitudinal historesin section of the non-decalcified DF growth cartilage. Alkaline phosphatase activity was found at the plasma membrane of the hypertrophic chondrocytes (arrows) and matrix calcification was detected by von Kossa's reactions (arrowheads). Methyl green counter-staining. Scale bar, 20μm.

Figure 14. 46-Stage tadpole. Longitudinal historesin section of the non-decalcified DF growth cartilage. Alkaline phosphatase activity was found at the plasma membrane of the chondrocytes since lower proliferative zone (lpz). Upper proliferative zone (upz). Methyl green counter-staining. Scale bar, 40μm.

Figure 15. Two-year-old animal. Longitudinal historesin section of the non-decalcified DF growth cartilage. Alkaline phosphatase activity (arrowheads) was found at the plasma membrane of the osteoblasts around a bone trabecula (bt). Methyl green counter-staining. Scale bar, 20μm.

Figure 16. Two-year-old animal. Longitudinal historesin section of the non-decalcified DF growth cartilage. Tartrate-resistant acid phosphatase activity was found in the cytoplasm (red staining) of a polynucleated osteoclast (oc) close to a bone trabeculae (bt) but also in contact with cartilage matrix (cm). Methyl green counter-staining. Scale bar, 10μm.

Figures 17: 46-Stage tadpole; **18:** 1-year-old animal; **19** and **20:** 2-year-old animal. DNA-fragmentation as revealed by TUNEL labeling. Positive reaction (arrows) was observed in chondrocytes within the three cell layer from the contact of the lower hypertrophic zone with the marrow in animals of the three age groups. Methyl green counter-staining. Scale bars, **17**= 20μm and **18-20** = 10μm.

Figure 21. TEM of one-year-old animal growth cartilage. Mononucleated cells (arrows) were found on the border of the bone marrow with the non-calcified cartilage matrix of the hypertrofic zone (hc). Scale bar, 3μm.

Figure 22. TEM of two-year-old animal growth cartilage. Matrix vesicles (arrows) were found in the extracellular matrix of the upper hypertrophic zone. Scale bar, 300nm.

Figure 23. TEM of two-year-old animal growth cartilage. Spherical structure of calcified cartilage matrix, isolated (short arrow) or coalesced (long arrows) were found in the lower hypertrophic zone. Scale bar, 2μm.

Figure 24. TEM of two-year-old animal growth cartilage. Multinucleated cell with many vesicles in the cytoplasm was found sunrounding two spherical structures of calcified matrix (asterisk) in the bone marrow. Nucleus (n). Scale bar, 3μm.

Table 1 . Events associated with the growth cartilage of the bullfrog at different ages

Event	Age		
	46-stage tadpole	**1-year-old animals**	**2-year-old animals**
Cell death	+	+	+
AlkPase activity	+	+	+
Matrix calcification	-	-	+
Endochondral ossification[1]	-	-	+

[1]Observed as the deposition of bone trabeculae on the surface of either calcified or uncalcified cartilage

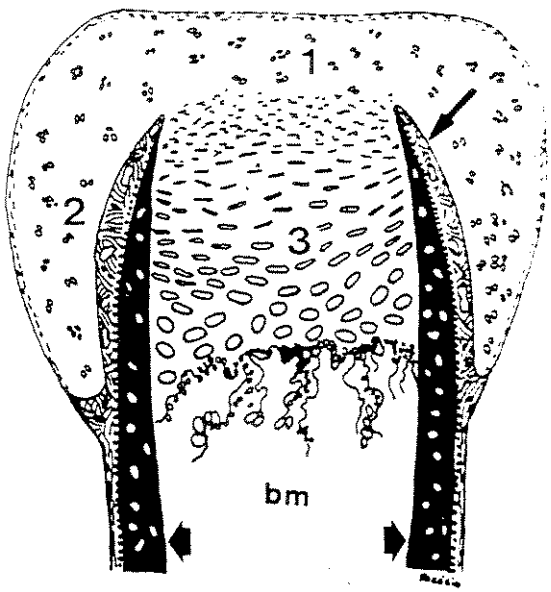

Figure 1.

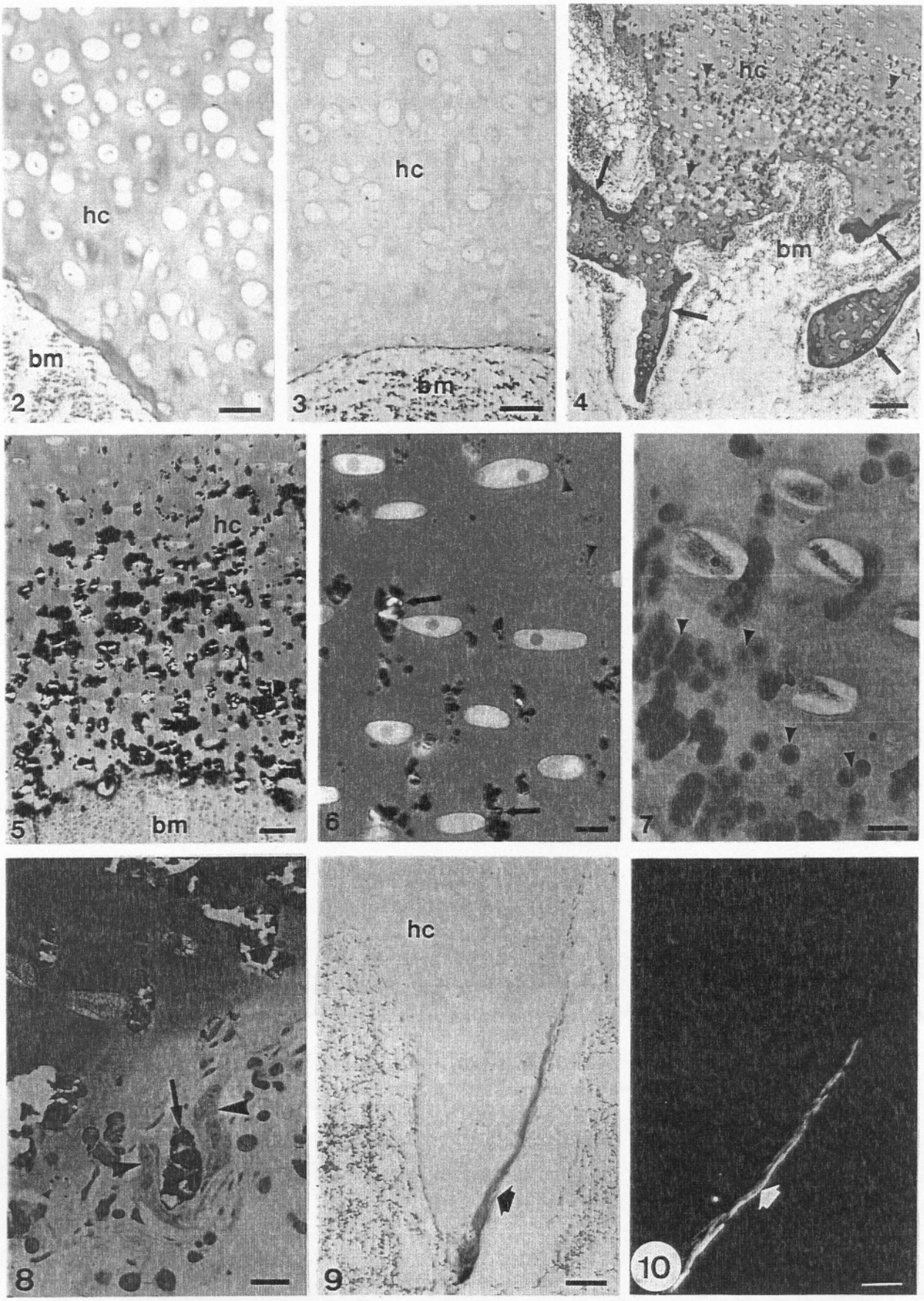
hc
bm
2
hc
bm
3
hc
bm
4
hc
bm
5
6
7
hc
8
hc
9
10

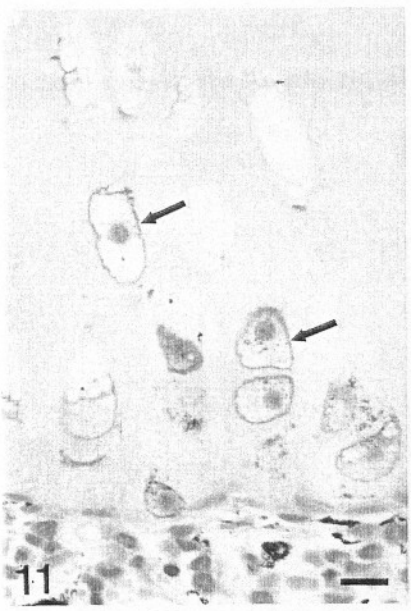
11

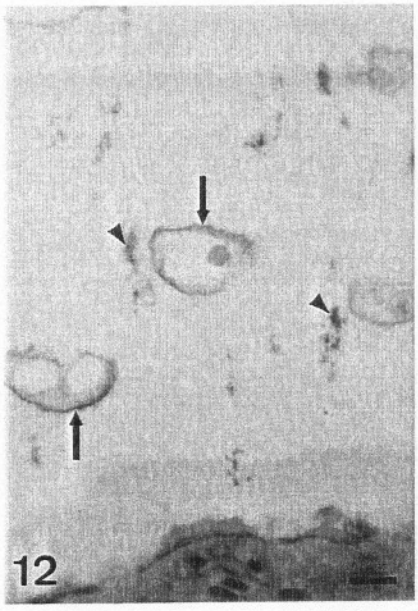
12

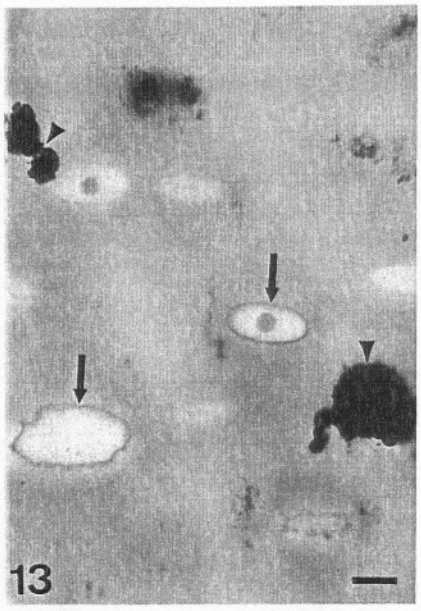
13

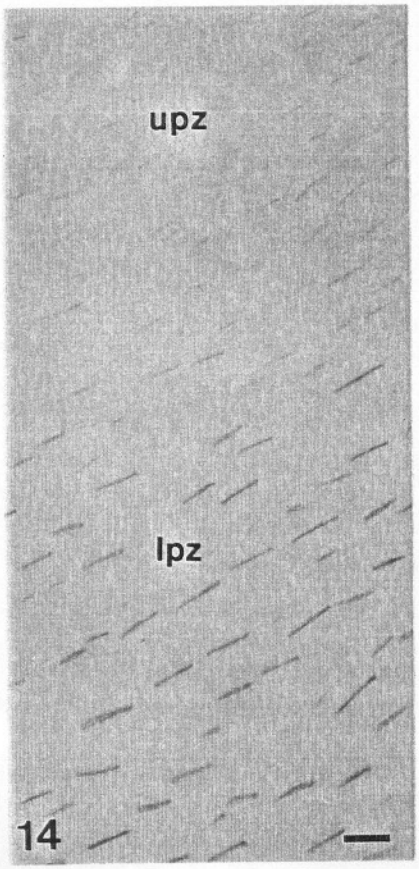

14

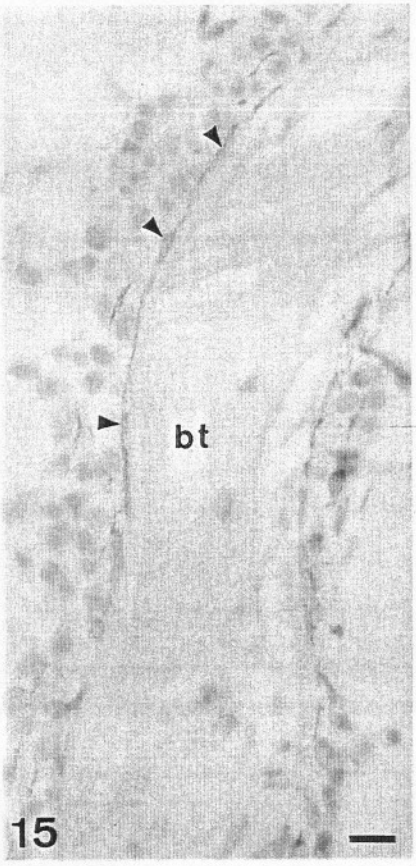

15

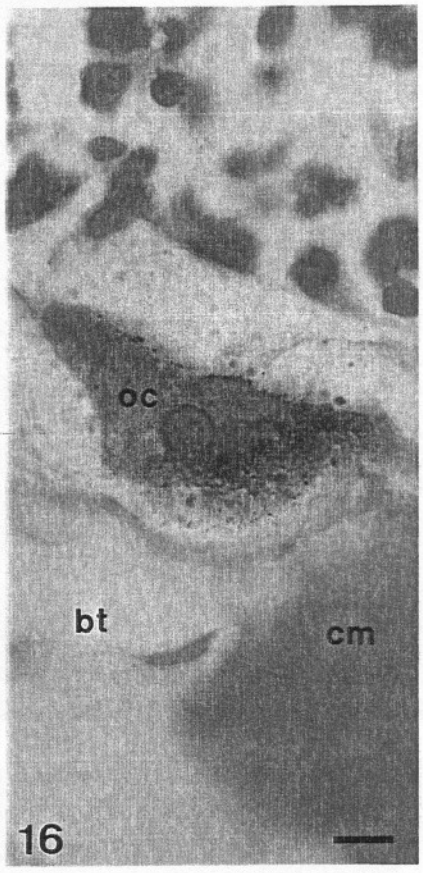

16

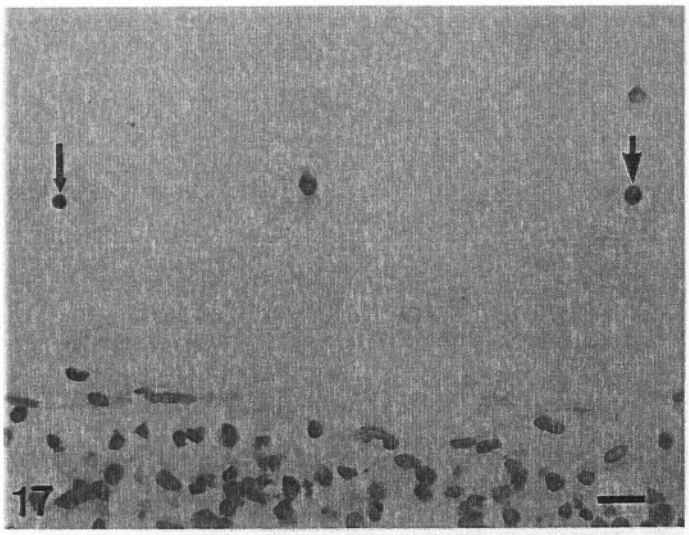
17

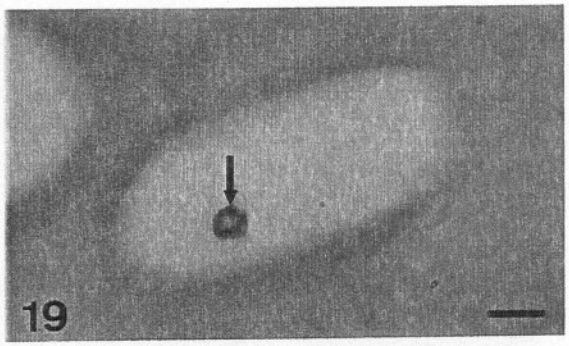
19

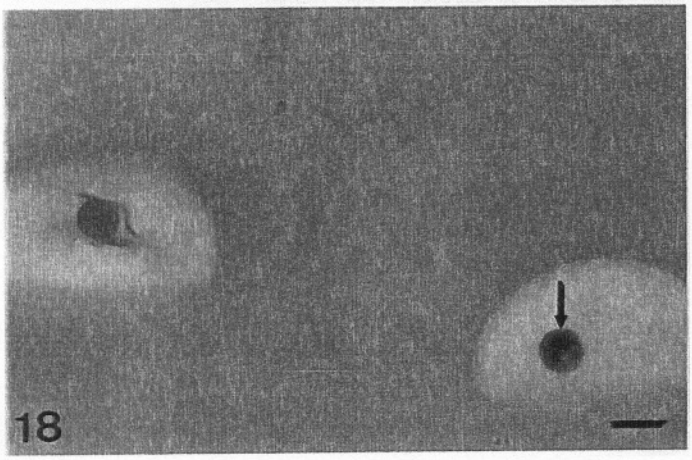
18

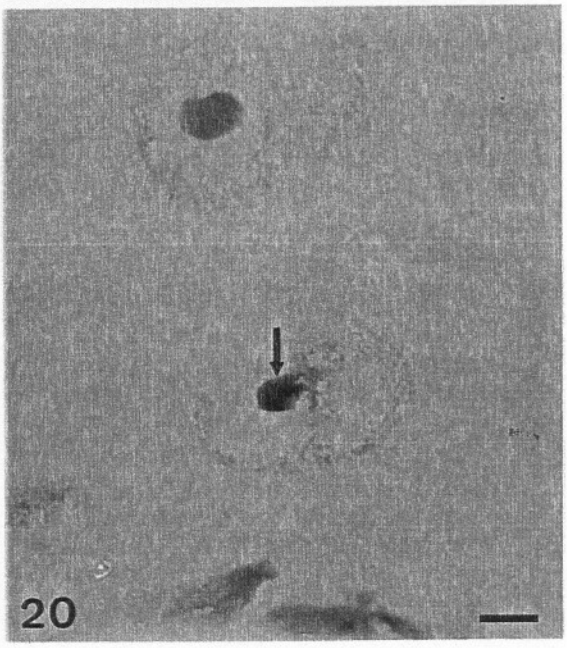
20

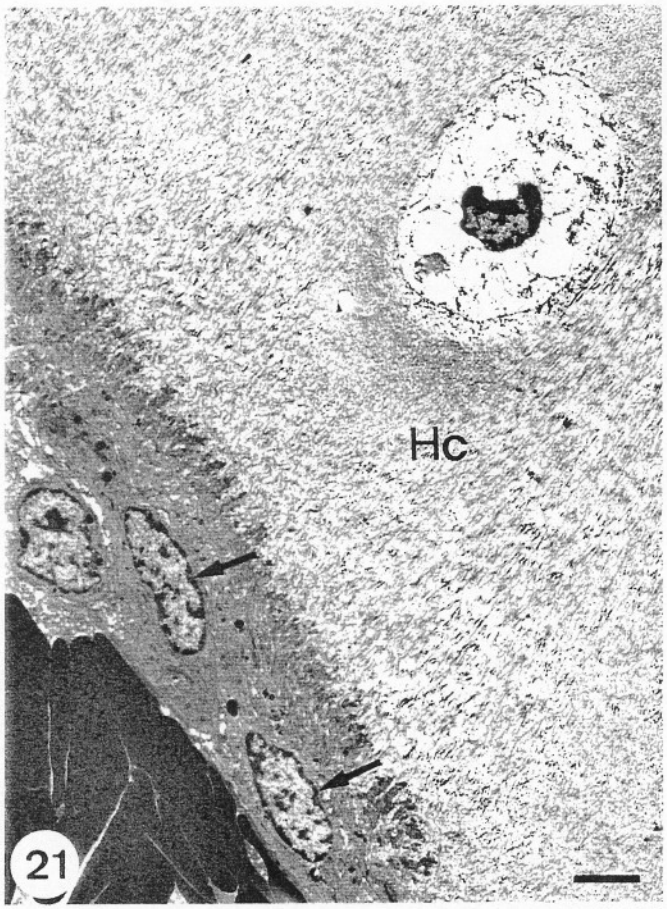
Hc
21

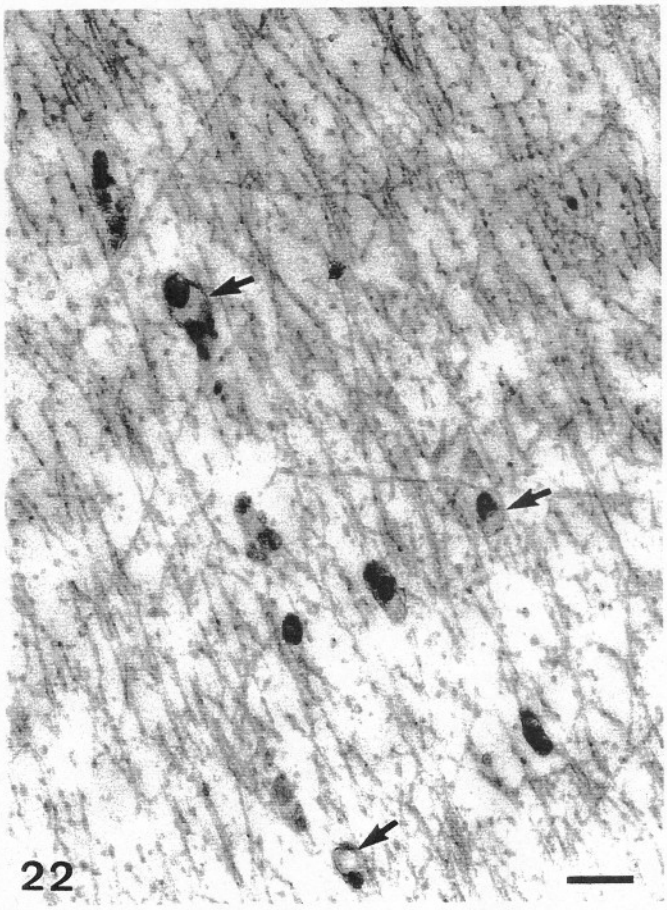
22

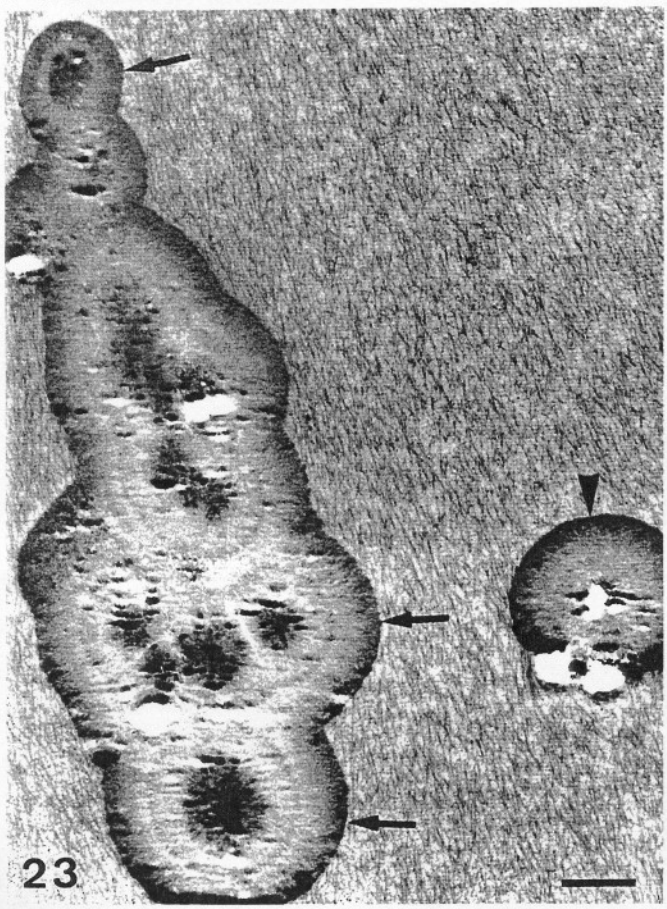
23

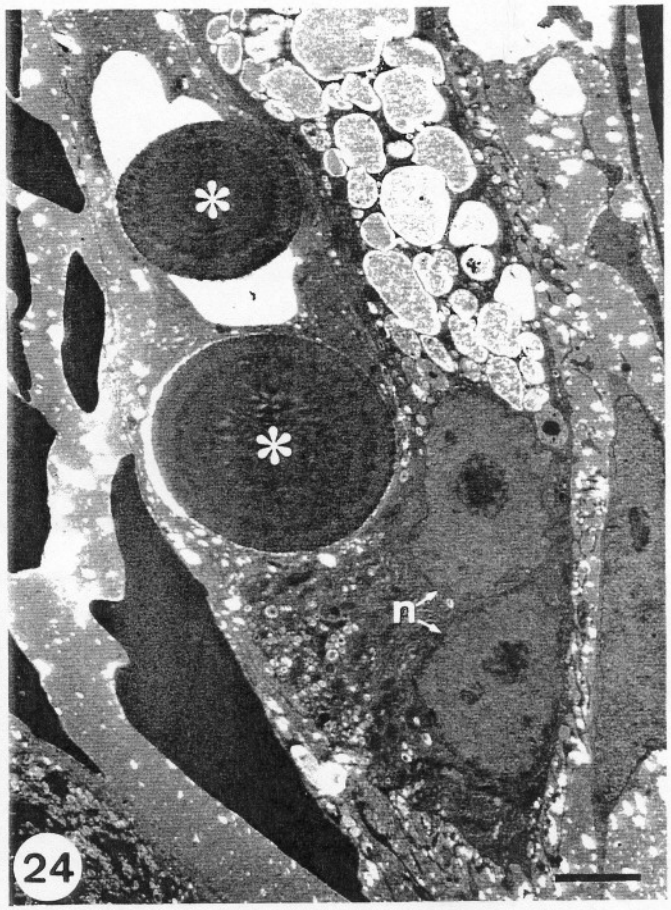
n
24

3.3 Ectopic calcification of articular cartilage in the bullfrog *Rana catesbeiana* and its possible involvement in bone closure. Submetido para publicação na revista Cell and Tissue Research

Abstract

Calcification of the articular cartilage is a pathological condition associated with age and certain joint diseases in humans and other mammals. In this work, we describe a physiological process of articular cartilage calcification in bullfrogs. Articular cartilage of the proximal and distal ends of the femur and of the proximal end of the tibio-fibula was studied in animals of different ages. Calcification of the articular cartilage was detected in animals at 1 month post-transformation. This calcification, which appeared before the hypertrophic cartilage showed any calcium deposition, began at a restricted site in the lateral expansion of the cartilage and then progressed to other areas of the epiphyseal cartilage. Calcified structures were identified by von Kossa´s staining and by *in vivo* incorporation of calcein green. Element analysis showed that calcium crystals were consisted of poorly-crystaline hydroxyapatite. Calcified matrix were initially spherical structures that generally coalesced after a certain size to occupy larger areas of the cartilage. Alkaline phosphatase activity was detected at the plasma membrane of nearby chondrocytes and in extracellular matrix. Apoptosis was detected by the TUNEL reaction in some articular chondrocytes from calcified areas. The area occupied by calcium crystals increased significantly in older animals, especially in areas under compression. Ultrastructural analyses showed clusters of needle-like crystals in the extracellular matrix around the chondrocytes and large blocks of calcified matrix. In 4-year-old animals, some lamelar bone (containing bone marrow) occurred in the same area as articular cartilage calcification. These results show that the articular cartilage of *R. catesbeiana* undergoes precocious and progressive calcification that is apparently stimulated by compressive forces. We suggest that this calcification is involved in the closure of bone extremities, since calcification appears to precede the formation of a rudimentary secondary center of ossification in older animals.

Introduction

Cartilage matrix calcification, an important and well regulated process in the hypertrophic zone of the growth plate, is associated with endochondral ossification (Hunziker, 1994; Elerbacher et al. 1995; Cancedda et al. 1995). In contrast, calcification of the articular cartilage matrix is a damaging process associated with some joint diseases because it disruptis the normal functioning of the cartilage matrix (Anderson, 1988; Schumacher, 1988; Ohira and Ishikawa, 1987).

Cartilage calcification can be stimulated by mechanical loading (van't Veen et al. 1995; Milz et al. 1997; Tanck et al. 1999), and alkaline phosphatase (AlkPase) activity, matrix vesicle production and chondrocyte apoptosis are involved in this process (Leboy et al 1989; Anderson 1995; Kim, 1995; Kirsch et al. 1997; Hashimoto et al. 1998).

There are important differences in the epiphyseal cartilage structure and its involvement in long bone growth between anurans and mammals (Felisbino and Carvalho, 1999; 2000). An interesting distinction in anurans involves the presence of a lateral expansion of the articular cartilage that covers some distance of the outer side of the tubular periosteal bone end. This expansion is probably an adaptation to these animal's resting position in which the knees are kept bent. Furthermore, endochondral ossification is a late process and hypertrophic cartilage calcification is only found in 2-year-old animals (Felisbino and Carvalho, submitted manuscript).

An additional feature of the articular cartilage in anurans is the presence of mineral deposits in young adults. Considering that the chemical nature of this accumulated material, the kinetics of its deposition and it relevance to physiological or pathological processes in articular cartilage are poorly understood, we decided to investigate some aspects of articular cartilage calcification of *Rana catesbeiana* using radiographic, physicochemical, histological and ultrastructural analyses. Our results demonstrate that a progressive, non-pathological, cell-mediated deposition of calcium phosphate (hydroxyapatite) occurs in the articular cartilage of post-transformation bullfrogs and that this process it may precede the formation of lamelar bone in very old animals and contribute to bone closure.

Materials and Methods

Animals

The hind limbs of tadpoles at different stages of development (Gosner, 1960) and of 1 month, 1 year, 2 year and 4 year post-transformation bullfrogs (*Rana catesbeiana*) were obtained from a farm in Atibaia (São Paulo State, Brazil). Animals from a farm in Sacramento (California, USA) were also examined in this study. Five males and five females were used for each age group. The animals were killed by decapitation after cold immobilization and the proximal femoral (PF), distal femoral (DF) and proximal tibio-fibula (PTF) epiphyseal cartilages were dissected out and immediately fixed.

Radiograph X ray analysis

A whole hind limb of one-year-old animal was dissected out and fixed for 24 h in 4% formaldehyde in phosphate buffered saline (PBS). The material was then washed and preserved in 20% ethanol until it was radiographed. The radiograph film was used to obtain a positive image of the sites of calcium accumulation.

Mineral characterization

Fragments of articular cartilage from one-year-old animal were dissected out and digested with 1% trypsin in 50 mM Tris-HCl buffer, pH 8.0, for 12 h at 37°C. The residue was washed several times with distilled water and part of it then dissolved in concentrated HCl. The calcium/phosphate ratio was determinated by ICP/AES (Inductive Coupled Plasma/Atomic Emission Spectroscopy). Another portion of the residue was characterized by X-ray diffraction.

Histology

Epiphyseal cartilages were fixed for two days in 4% formaldehyde in PBS. Some samples were decalcified in a 4% formaldehyde, 10% acetic acid and 0.85% NaCl solution for 15 days or in PBS containing 15% EDTA for 3 days. The material was then dehydrated in a graded ethanol series, clarified in Cedar wood oil, embedded in Paraplast-Plus embedding medium and sectioned at 6 μm. Some fragments were embedded in JB-4 resin (Polysciences Inc.) and sectioned at 2 μm. Sections were subjected to the von Kossa's reaction for calcium deposits or stained with hematoxylin and eosin (HE).

Calcein green incorporation

Some animals were given a subcutaneous injection of calcein green (50 mg/kg body weight) (Kimpel et al. 1999). Two injections was administered at an interval of 5 days. The animals were maintained for 5 days after the last dose and then sacrificed. The cartilage samples were mounted in Tissue Tek, frozen in liquid nitrogen, and sectioned in a Microm cryostat. Sections (7 μm) were collected in silanized glass slides, fixed with cold 4% paraformaldehyde in PBS, washed and mounted in VectaShield (Vector Labs. Inc., Burlingane CA, USA). The preparations were observed with either a Zeiss Axioskop or an Olimpus fluorescence microscope.

Enzyme histochemistry

Tissue fragments were fixed in 4% formaldehyde in 0.1 M cacodylate buffer at pH 7.2 for 4 h, washed with the same buffer, soaked in 70% ethanol and embedded in JB-4 resin. Two micrometer thick sections were assayed for alkaline phosphatase (AlkPase) activity using 0.1% α-naphtyl phosphate, 0.1% fast red and 50 mM $MgCl_2$ in 0.1 M Tris-malate buffer, pH 10.0. Controls were run in the same solutions without α-naphtyl phosphate (Bancroft 1982; Cole and Wezeman 1987). Sections were counter-stained with methyl-green and mounted in 80% glycerol.

DNA fragmentation

DNA fragmentation was detected by *in situ* labeling with the terminal deoxynucleotidyl transferase method (TdT-FragEl - Amersham-Phamacia). Paraplast sections were treated with proteinase K and 3'-end labeled with biotin-conjugated dUTP. An incubation step with peroxidase-conjugated streptavidin was followed by the DAB reaction. Sections were counter-stained with methyl green. Negative controls were obtained by omitting the enzyme from the incubation solution and a positive control was produced by previous digestion with DNase I.

Transmission electron microscopy (TEM)

Selected areas of the epiphyseal cartilage from one-year-old bullfrogs were processed for TEM. Tissue fragments (1 mm^3) were fixed with 3% glutaraldehyde plus 0.25% tannic acid in Millonig's buffer containing 0.54% glucose (Cotta-Pereira et al. 1976). Tannic acid was chosen for better preservation and visualization of the fibrillar components. After washing with the same buffer, the material was post-fixed with 1% osmium tetroxide, washed again, dehydrated in

graded acetone, and embedded in Epon 812. Ultrathin silver sections were cut using a diamond knife on a LKB ultramicrotome and contrasted with alcoholic uranyl acetate and lead citrate. Grids were examined in a Leo 906 transmission electron microscope operating at 80 kV.

Results

The epiphyseal cartilage of the distal femoral end of *Rana catesbeiana* was formed by a large mass of hyaline cartilage attached to the extremity of the periosteal bone shaft and showed three regions: (1) the articular cartilage proper, (2) the lateral articular cartilage, and (3) the growth cartilage. The epiphyseal cartilage was inserted into the periosteal bone and the inner surface of the lateral articular cartilage was attached to the external surface of the periosteal bone by a fibrous tissue, the osteochondral ligament (OCL) (Fig. 1).

Radiographic imaging showed the presence of crystal deposits in the articular cartilage of the femur and tibio-fibula extremities (Figs. 2-4). Analysis of the inorganic material from the calcified cartilage showed that the calcium: phosphate ratio was 1.63, close to the value for hydroxyapatite (1.67). X-Ray diffraction analyses revealed poorly-crystaline hydroxyapatite (data not shown).

There was no calcification of the articular cartilage in any tadpole before transformation. However, after transformation, all animals showed some degree of calcification of the articular cartilage. There was no difference between the Brazilian and American specimens of *R. catesbeiana* examined.

In animals sacrificed 30 days after transformation, the von kossa's reaction produced positive staining in the periosteal bone matrix and in some areas of the lateral articular cartilage, mainly in a region adjacent to the osteochondral ligament (Fig. 5). This reaction occurred in the lateral articular cartilage of the PF, DF and PTF and occupied a increasing area in older animals (Fig. 6). The accumulation of positive von Kossa material was more prominent in areas of contact between the bone extremities inside the joints.

AlkPase activity was present on the surface of chondrocytes of the lateral articular cartilage and also in the extracellular matrix. This activity was restricted to the chondrocytes and matrix closest to the calcified areas (Figs. 7 and 8).

Calcein green incorporation was intense in periosteal bone and in the calcified matrix of the lateral articular cartilage (Figs. 9 and 10). At 30 days post-transformation, the stained area

was restricted to the articular cartilage adjacent to the periosteal bone and was more intense on the sides of contact between the bone ends (Fig.9). There was a progressive accumulation of calcium deposits as the animals aged (Fig. 10). Calcein labeling also spread to other areas of the articular cartilage. Higher magnification of the calcein green incorporation revealed the presence of spherical structures that appeared isolated or fused with each other around the larger calcium deposits (Figs. 11 and 12).

Ultrastructural observations showed isolated or aggregated clusters of needle-like crystals around the calcified matrix and chondrocytes of the lateral articular cartilage (Fig. 13). A more detailed analysis of the needle-like crystals suggested that they grew from the center outwards (Fig.14).

A positive reaction for DNA fragmentation was obtained in some chondrocytes of the lateral articular cartilage from animals at different post-transformation ages (Figs. 15-18). Treatment with DNase I produced a positive reaction in all cell nuclei (Fig.19).

Lamelar bone delimiting the marrow cavities was observed in 4-year-old bullfrogs at the sites of calcium deposition seen in younger animals (Fig. 20).

Discussion

The epiphyseal cartilage of *R. catesbeiana* showed distinct structural features compared to corresponding mammalian and avian tissue (Felisbino & Carvalho 1999). This cartilage inserted at the end of a tubular bone and, given the absence of endochondral bone in adults stage, the attachment to the bone was provided by the osteochondral ligament, a specialized fibrous structure that anchors the lateral articular cartilage to the outer surface of the bone (Felisbino & Carvalho, 2000). In contrast, the aggrecan molecule found in bullfrog cartilage shows many similarities to mammalian and avian aggrecans (Covizi & Carvalho, 2000).

Although calcification sites are present in the epiphyseal cartilage of other anuran species (Haines, 1942; Mopty & Cimarosty, 1979; Dikson, 1982; Dell'Orbo et al. 1992), the inorganic composition of the matrix, the pattern of calcification and the cellular aspects involved in calcium deposition have not been studied.

Based on the calcium: phosphorus ratio and on the diffractogram, the inorganic matrix was an poorly-crystaline hydroxyapatite, which starts to accumulate after metamorphosis when the animal adopts amphibian behavior. Calcium deposition begins in the lateral cartilage and

progresses towards the articular cartilage in an ordered manner, as indicated by the study of animals at different ages. The calcium deposits later appear to coalesce to close the tubular bone end. In addition, the calcified matrix is at least partially replaced by bone trabeculae and marrow in old animals.

AlkPase activity and programmed cell death were detected at the sites of calcification. AlkPase is constantly expressed during the proliferation, maturation and hypertrophy of chondrocytes in hypertrophic cartilage of the bullfrog (Felisbino & Carvalho, submitted manuscript). We have also detected AlkPase activity in chondrocytes and in the extracellular matrix close to the calcification areas of articular cartilage, which may reveal its participation in calcification events.

Apoptotic chondrocytes were rare and restricted to calcified areas of articular cartilage of adult animals, while no DNA fragmentation was detected in the corresponding areas of swimming tadpoles, which also showed no calcium deposition.

Even though this association between apoptotic chondrocyte and calcification is clear in the articular cartilage, in bullfrog hypertrophic cartilage, such an association is not so clear since DNA fragmentation was detected in hypertrophic chondrocytes that were not associated with matrix calcification (Felisbino & Carvalho, submitted manuscript).

The relationship between apoptosis and calcification remains unclear, since Adams and Horton (1998) reported apoptosis in chondrocytes of uncalcified articular cartilage in mice and noted that the number of apoptotic cells increased with age, whislt some authors have suggested that matrix vesicles are apoptotic bodies of dying chondrocytes (Kim, 1995). On the other hand, this association seems to be relevant in pathological conditions (Hashimoto et al. 1998).

Calcein green incorporation provided complementary results to those revealed by von Kossa's reaction. The spherical structures labeled with calcein green were not seen in von Kossa's reaction but their growth pattern indicated that calcification occurs in some nuclei with concentric growth and subsequent fusion to form larger calcified areas. Ultrastructural analysis confirmed that needle-like crystals start growing from a nucleus. Whether this nucleus corresponds to a matrix vesicle released by chondrocytes was not defined in this work.

The calcification of articular cartilage in the bullfrog contributes to the formation of bony trabeculae lining marrow cavities in 4-year-old animals, in an arrangement somewhat similar to the mammalian secondary center of ossification. However, while in mammals the formation of

secondary centers of ossification begins with cartilage invasion by cartilage canals, the hypertrophy of chondrocytes and matrix calcification (Roach et al. 1998), in *R. catesbeiana*, calcification precedes the invasion by blood vessels and no chondrocyte hypertrophy is observed.

The moment of transition from calcified matrix to bone formation, characterized by the deposition of bone on the surface of the mineralized matrix by osteoblasts, was not observed. However, the bone trabeculae found in 4-year-old animals occupied regions of articular cartilage that were calcified in young adults.

We believe that compressive stimulation for cartilage calcification occurs during the joint movements necessary for jumping or even during resting position. This idea is reinforced by the fact that swimming tadpoles had already the lateral articular cartilage formed and did not show any sign of calcification. Additionally, soluble factors acting on osteoblasts to stimulate bone growth could affect chondrocytes of the lateral articular cartilage, and this effect could be potentiated by mechanical stimulation.

In conclusion, the articular cartilage of *R. catesbeiana* is calcified after metamorphosis. Hydroxyapatite is progressively deposited in the lateral cartilage and then in the articular cartilage proper. Crystals grow from a nucleus to form large areas of mineralized matrix. The initiation of calcification is apparently controlled by chondrocytes that express AlkPase and die by programmed cell death. Since calcification occurred in an ordered fashion, appeared in all post-transformation animals and lead to the closure of the tubular bone end, it seems that this process must involve mechanical stimulation.

References

Adams CS, Horton Jr. WE (1998) Chondrocyte apoptosis increases with age in the articular cartilage of adult animals. Anat Rec 250: 418-425

Anderson HC (1988) Mechanism of pathologic calcification. Rheum Dis Clin North Am 14: 303-315

Anderson HC (1995) Molecular biology of matrix vesicles. Clin Orthop 34: 266-280

Bancroft JD (1982) Enzyme histochemistry. In: Bancroft JD, Stevens A (eds) Theory and Practice of Histological Techniques. Churchill Livingstone. Edinburgh pp 384-387

Cancedda R, Cancedda FD, Castagnola P (1995) Chondrocyte differentiation. Int Rev Cytol 159: 265-359

Cole AA, Wezeman FH (1987) Cytochemical localization of tartrate-resistant acid phosphatase, alkaline phosphatase, and nonspecific esterase in perivascular cells of cartilage canals in the developing mouse epiphysis. Am J Anat 180: 237-242

Cotta-Pereira, G., Rodrigo, F.G. and David-Ferreira, J.F. 1976. The use of tannic acid-glutaraldehyde in the study of elastic related fibers. Stain Technol., 51, 7-11.

Covizi DZ, Carvalho HF (2000) Aggrecan structure in amphibian cartilage. Braz J Med Biol Res 33: 1403-1412

Dell'Orbo C, Gioglio L, Quacci D (1992) Morphology of epiphyseal apparatus of a ranid frog. Histol Histopathol 7: 267-273

Dikson RG (1982) Ultrastruture of growth cartilage in the proximal femur of the frog, *Rana temporaria*. J Anat 135: 549-564

Elerbacher A, Filvaroff EH, Giltelman SE and Derynck R (1995) Toward a molecular understanding of skeletal development. Cell 80: 371-378

Felisbino SL, Carvalho HF (1999) The epiphyseal cartilage and growth of long bones in *Rana catesbeiana*. Tissue Cell 31: 301-307

Felisbino SL, Carvalho HF (2000) The osteochondral ligament of *Rana catesbeina*: a fibrous attachment between bone and articular cartilage. Tissue Cell 32: 527-536

Gosner KL (1960) A simplified table for staging Anura embryos and larvae with notes on identification. Herpetologica 16: 183-190

Haines RW (1942) The evolution of epiphyses and of endochondral bone. Biol Rev 17: 267-292

Hashimoto S, Ochs RL, Rosen F, Quach J, McCabe G, Solan J, Seegmiller JE, Terkeltaub R, Lotz M (1998) Chondrocyte-derived apoptotic bodies and calcification of articular cartilage. Proc Natl Acad Sci USA 95: 3094-3099

Hunziker EB (1994) Mechanism of longitudinal bone growth and its regulation by growth plate chondrocytes. Microsc Res Tech 28: 505-519

Kim KM (1995) Apoptosis and calcification. Scannig Microsc 9: 1137-1178

Kimpel M, Claassen H, Fleiner B, Tillmann B (1999) Vascularization and cartilage mineralization of the thyroid cartilage of Munich minipigs and domestic pigs. Anat Embryol 199: 281-290

Kirsch R, Nah HD, Shapiro IM, Pacifici M (1997) Regulated production of mineralization-competent matrix vesicles in hypertrophic chondrocytes. J Cell Biol 137: 1149-1160

Leboy PS, Vaias L, Uschmann B, Golub E, Adams SL, Pacifici M (1989) Ascorbic acid induces alkaline phosphatase, type X collagen, and calcium deposition in cultured chick chondrocytes. J Biol Chem 264: 17281-17286

Milz S, Eckstein F, Putz R (1997) Thickness distribution of the subchondral mineralization zone of the trochlear notch and its correlation with the cartilage thickness: an expression of functional adaptation to mechanical stress acting on the humeroulnar joint? Anat Rec 248: 189-197

Roach HI, Baker JE, Clarke NMP (1998) Initiation of the bony epiphysis in long bones: chronology of interactions between the vascular system and the chondrocytes. J Bone Miner Res 13: 950-961

Schumacher RH (1988) Pathology of crystal deposition diseases. Rheum Dis Clin North Am 14: 269-302

Ohira T, Ishikawa K (1987) Hydroxyapatite deposition in osteoarthritic articular cartilage of the proximal femoral head. Arthritis Rheum 30: 651-660

Tanck E, van Driel WD, Hagen JW, Burger EH, Blankevoort L, Huiskes R (1999) Why does intermittent hydrostatic pressure enhance the mineralization process in fetal cartilage? J Biomech 32: 153-161

van't Veen SJ, Hagen JW, Van Ginkel FC, Prahl-Andersen B, Burger EH (1995) Intermittent compression stimulates cartilage mineralization. Bone 17: 461-465

Figure legends

Figure 1. Schematic drawing of the distal femoral epiphyseal cartilage of an adult *R. catesbeiana*. The epiphyseal cartilage was divided into: articular cartilage (1), lateral articular cartilage (2) and growth cartilage (3). The short arrows indicate the periosteal bone and the long arrow, the osteochondral ligament. **bm** - bone marrow. (Reprinted from Tissue & Cell, 31: 301-307. Felisbino & Carvalho, 1999, by permission of Churchill Livingstone.)

Figure 2. Radiograph imaging of mineral deposits in the femur (FE) and tibio-fibula (TF) of a 1 year post-transformation bullfrog. The hind limb was exposed to the X-ray beam in a lateral position.

Figure 3. Detail of the radiograph of the proximal femur showing sites of mineral deposition in the articular cartilage (arrowheads).

Figure 4. Detail of the distal femur (df) and proximal tibio-fibula (ptf), showing the sites of mineral deposition in the articular cartilage (arrowheads).

Figure 5. Von Kossa's reaction in a coronal section of the knee joint (distal femur = DF and proximal tibio-fibula = PTF) of an animal 30 days post-transformation. A positive reaction was observed in the periosteal bone (short arrows) and in the lateral articular cartilage (arrowheads) adjacent to the osteochondral ligament (OCL). X50.

Figure 6. Von Kossas reaction in a longitudinal section of distal femoral epiphyseal cartilage from a 2 year post-transformation animal. Note the positive black reaction in the periosteal bone (short arrow) and in the lateral articular cartilage (long arrows) close to the osteochondral ligament (OCL). X50.

Figure 7. Coronal section of distal femoral epiphyseal cartilage from an animal 30 day post-transformation. AlkPase activity was detected on the surface of some chondrocytes (arrows) and in the extracellular matrix (arrowheads) surrounding a calcified area (star) of the lateral articular cartilage. Osteochondral ligament (OCL). X200.

Figure 8. Coronal section of distal femoral epiphyseal cartilage from a 2-year-old post-transformation animal. AlkPase activity was detected at the plasma membrane of some chondrocytes (arrows) and in the extracellular matrix (arrowheads) surrounding a calcified area (stars) of the lateral articular cartilage. Osteochondral ligament (OCL). X200.

Figure 9. Coronal frozen section of distal femoral epiphyseal cartilage from an animal 30 day post-transformation. Calcein green incorporation appears as a strong yellowish-green fluorescence in periosteal bone (short arrows) and in the lateral articular cartilage (arrows). Note that calcium deposition is more prominent in the area of contact between the bone ends inside the joint. X50.

Figure 10. Coronal frozen section of distal femoral epiphyseal cartilage from an animal 2 years post-transformation. Calcein green incorporation occurred in the periosteal bone (short arrow) and in the lateral articular cartilage (arrows). The amount of calcein incorporation in the lateral articular cartilage was greater than in younger animals. X50.

Figure 11-12. Detail of figure 10 showing the spherical structures that appeared close to the calcified matrix (arrows). Fig. 11 = X200 and Fig. 12 = X400.

Figure 13. TEM of larteral articular cartilage from a one-year-old animal. Note the block of calcified matrix (CM) surrounded by clusters of needle-like crystals (arrows) close to healthy chondrocytes (CH). X5,000.

Figure 14. TEM of an isolated cluster of crystals showing the needle-like electron-dense structures (arrows) and collagen fibrils (arrowheads). X85,000.

Figures 15-19. Positive reaction for DNA fragmentation in the nuclei (arrows) of some chondrocytes close to the calcified cartilage matrix in an animal 30 day post-transformation (Fig. 16), a 1-year-old post-transformation animal (Fig. 17), a 2-year-old post-transformation animal (Fig. 18) and a 4-year-old post-transformation animal (Fig. 19). Figure 19 is positive control obtained by DNase I digestion of a tissue section from a 4-year post-transformation animal, showing that all nuclei were labeled (arrows). X400.

Figure 20. Longitudinal section of distal femoral epiphyseal cartilage from a 4-year-old post-transformation animal. Bone trabeculae (arrows) delimiting the bone marrow (bm) elements appeared in calcified lateral articular cartilage. pb - Periosteal bone. X50.

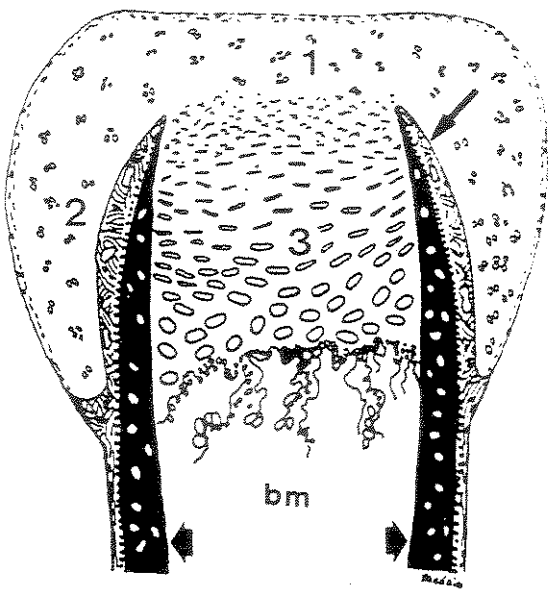

Figure 1.

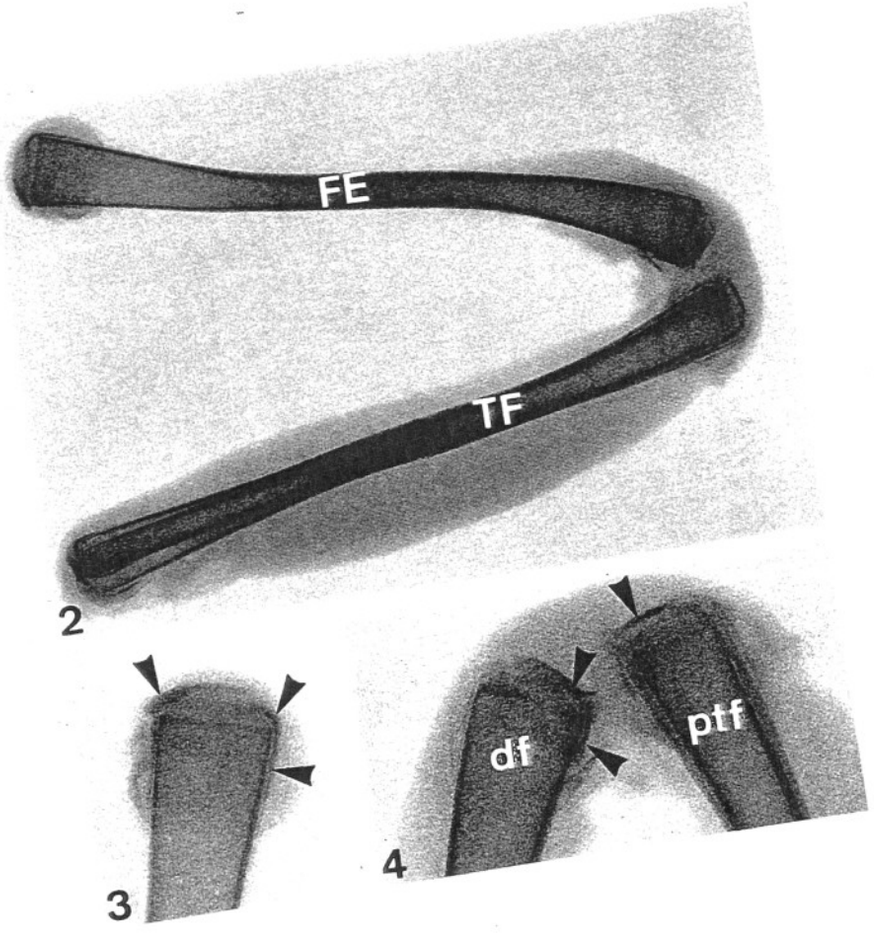
FE
TF
2
3
df
ptf
4

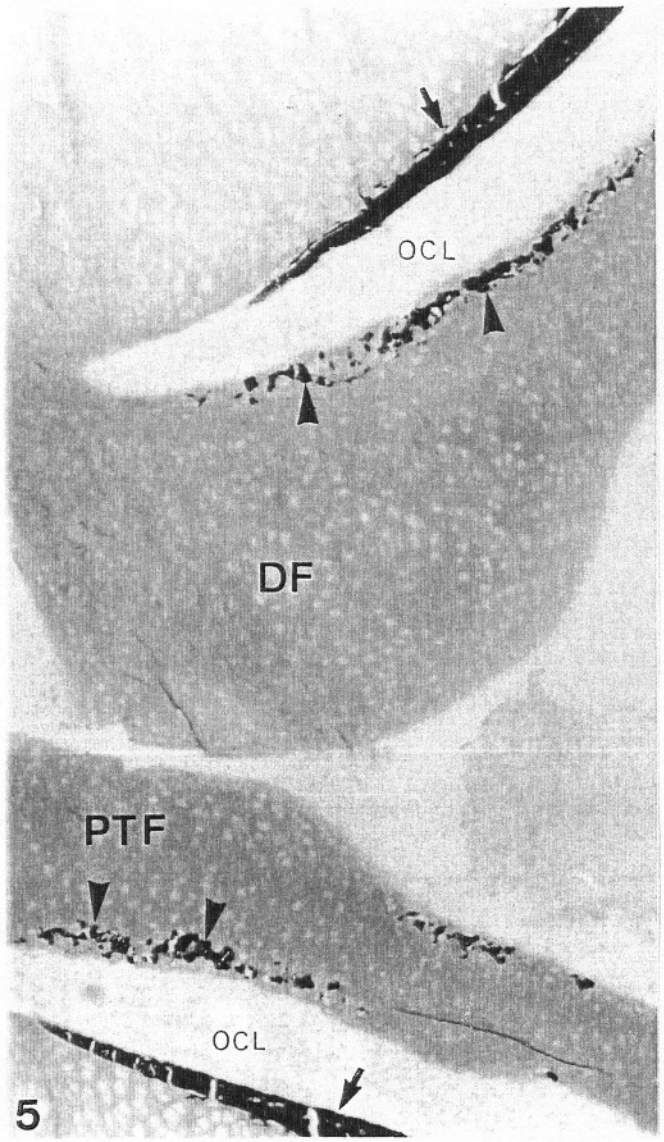
OCL
DF
PTF
OCL
5

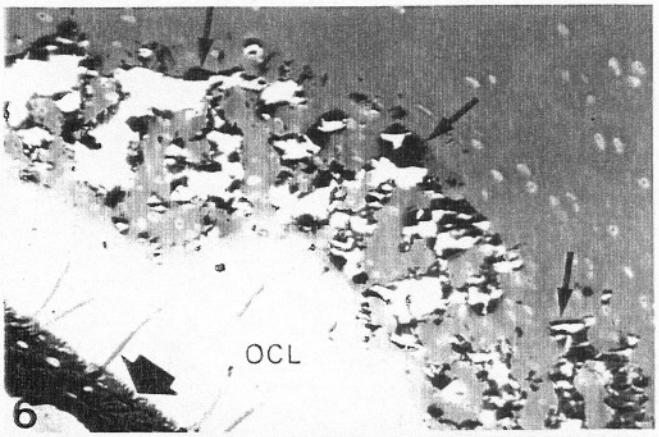
OCL
6

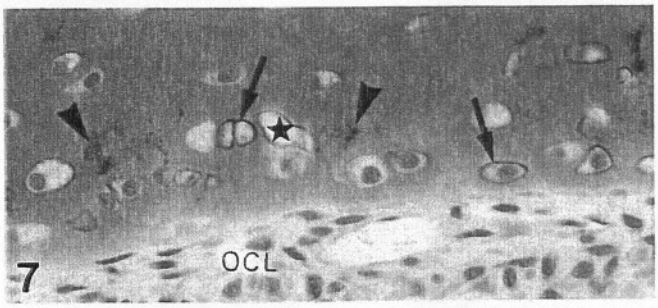
OCL
7

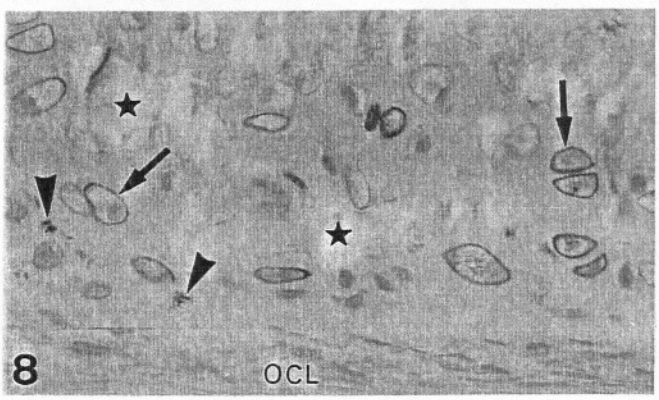
OCL
8

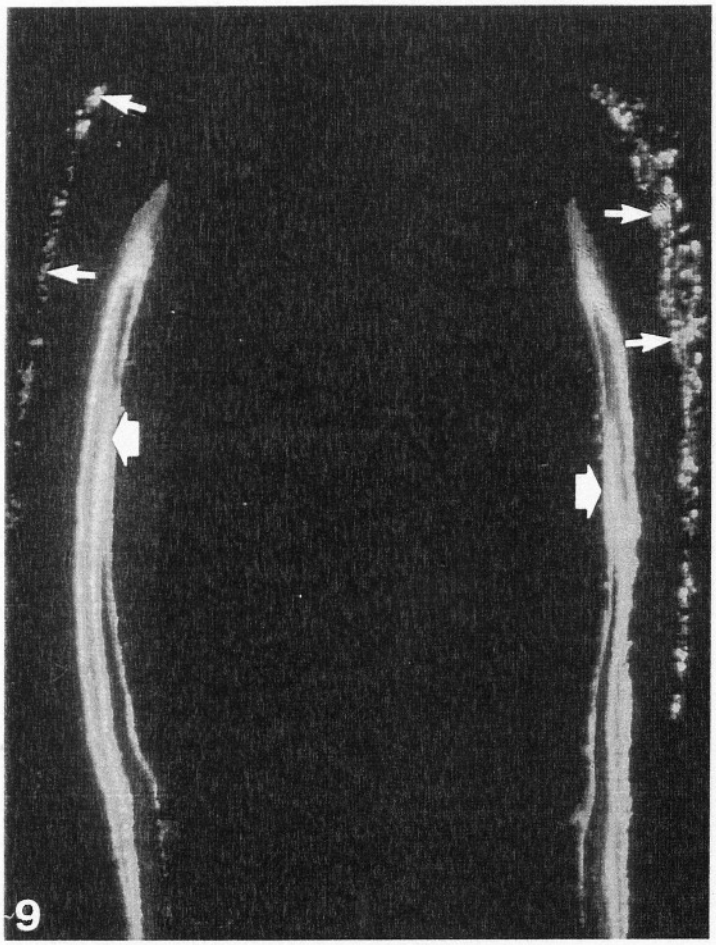

9

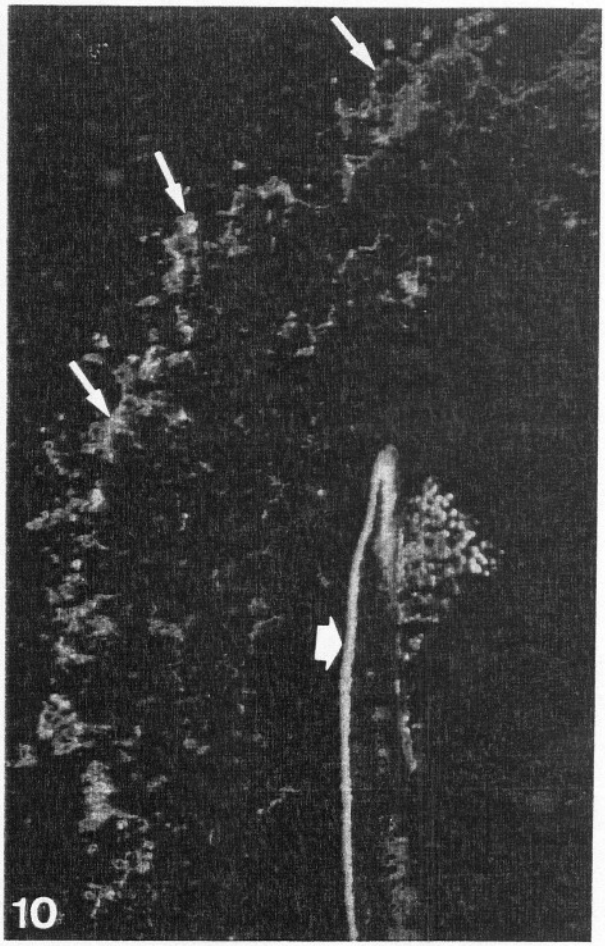

10

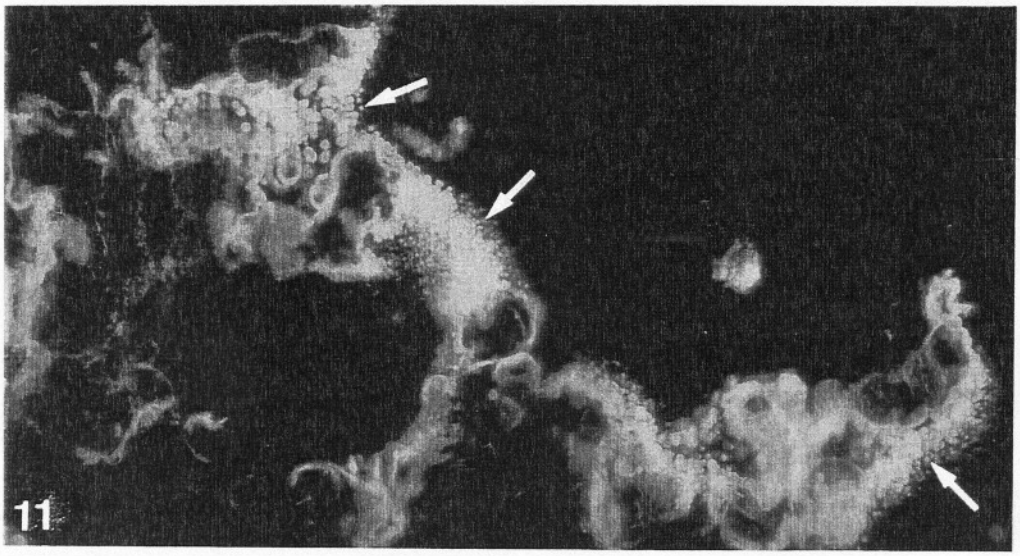

11

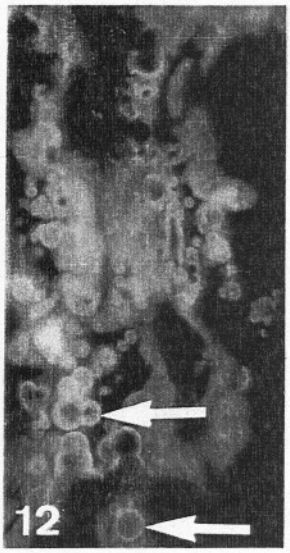

12

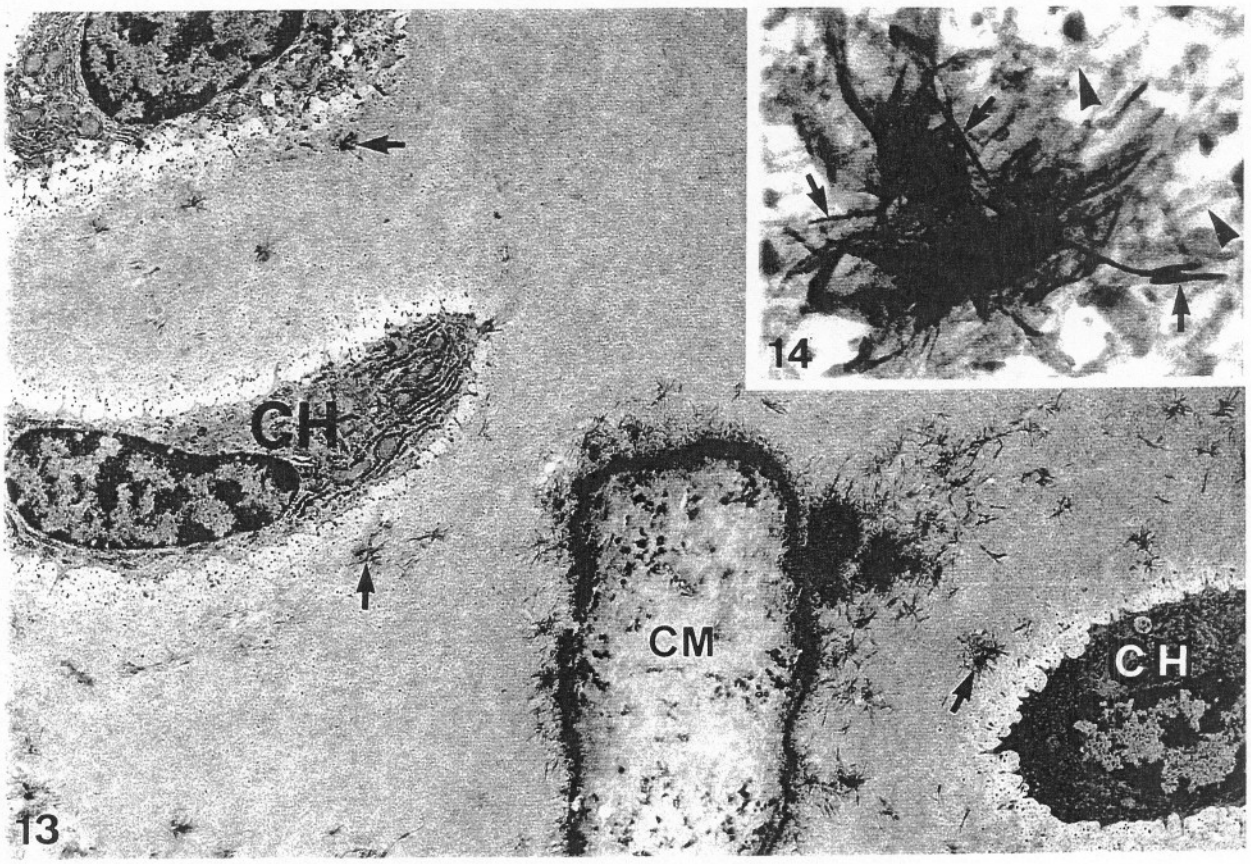
CH
CM
CH
13
14

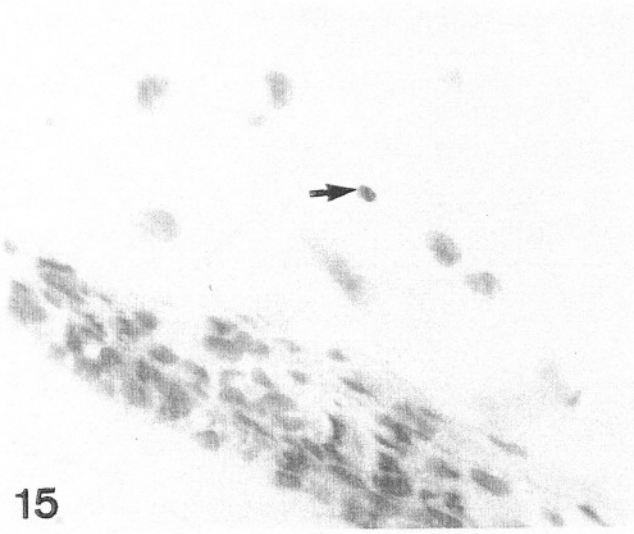

15

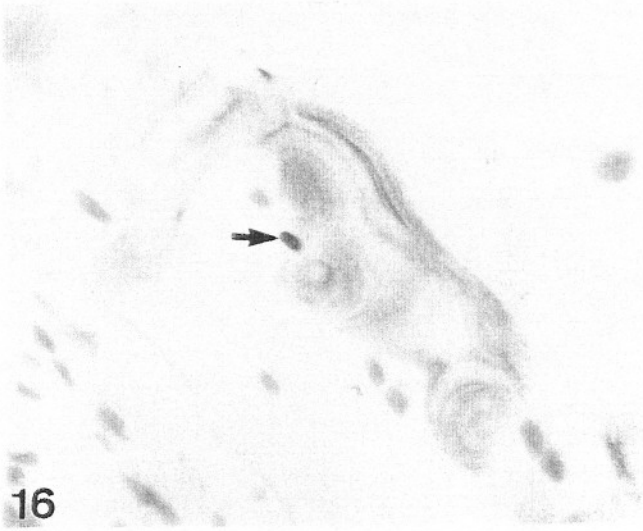

16

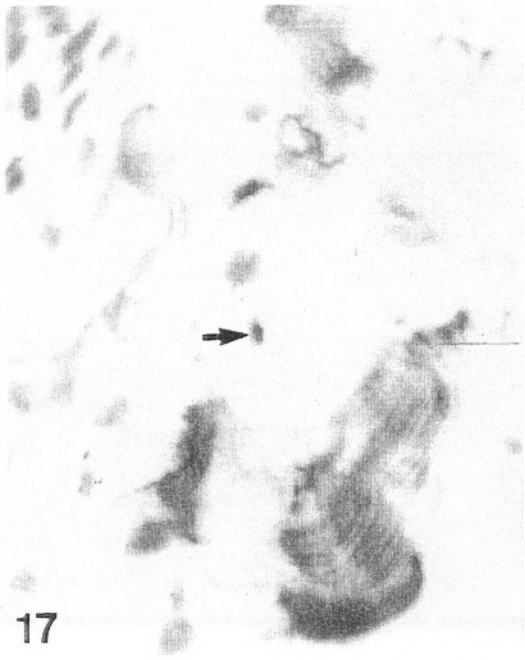

17

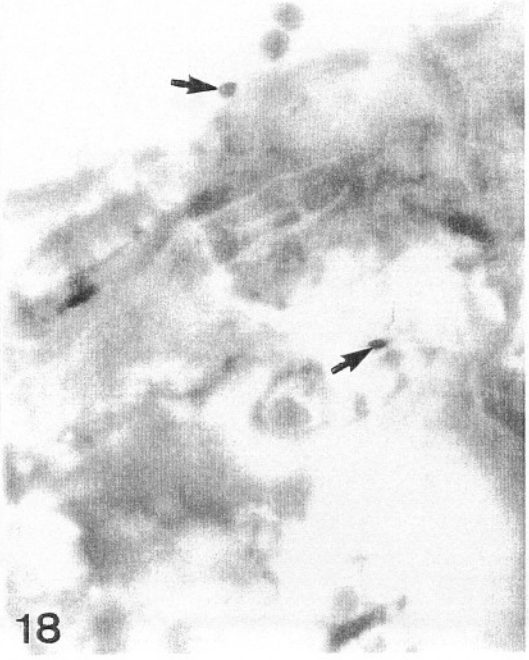

18

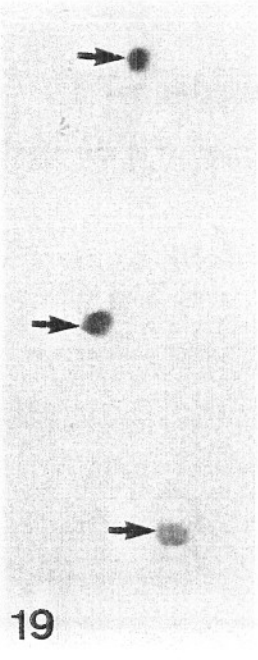

19

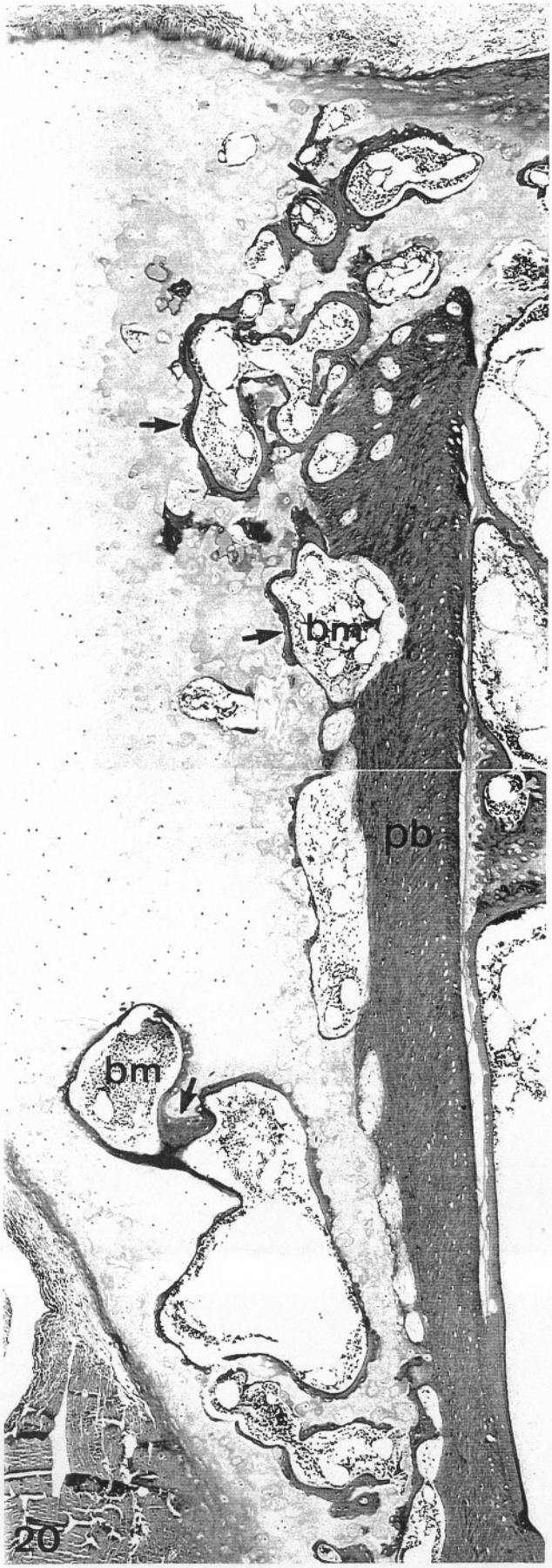
bm
pb
bm
20

4. Considerações finais

Os resultados deste trabalho permitem concluir que, em *Rana catesbeiana*:

1. Existe uma estrutura fibrosa complexa e especializada, denominada ligamento osteocondral, responsável por uma firme e flexível ancoragem da cartilagem articular à extremidade óssea e pelo crescimento ósseo longitudinal e radial.

2. O ligamento osteocondral é constituído de duas regiões distintas, com células e matriz extracelular diferenciadas, exibindo um arranjo de fibras de colágeno e de células semelhante ao ligamento periodontal.

3. A calcificação da cartilagem hipertrófica e a formação de trabéculas ósseas não estão presentes durante o desenvolvimento e crescimento ósseos. Nestes animais, o crescimento ocorre por ossificação periosteal essencialmente.

4. A calcificação da cartilagem hipertrófica e a formação de trabéculas ósseas aparecem nos animais mais velhos e podem estar relacionadas ao reforço das extremidades ósseas quando os animais ganham peso. Entrentanto, ambos os processos são independentes entre si.

5. Na cartilagem de crescimento, a atividade de fosfatase alcalina é constitutiva e só a sua atividade não é suficiente para produzir a calcificação da cartilagem hipertrófica.

6. A apoptose dos condrócitos hipertróficos não é causa nem conseqüência da calcificação, mas faz parte da programação destas células.

7. A absorção da cartilagem hipertrófica não calcificada é feita por células mononucleadas. Já a matriz de cartilagem calcificada e as trabéculas ósseas são absorvidas por osteoclastos.

8. A calcificação da cartilagem articular é um processo comum, não patológico e mediado pelas células.

9. A calcificação é, aparentemente, iniciada pela ação de forças de compressão que passam a existir após a metamorfose.

10. A atividade de fosfatase alcalina nos condrócitos da cartilagem articular parece estar diretamente relacionada à calcificação.

11. O componente inorgânico da matriz calcificada da cartilagem articular é constituído de uma hidroxiapatita pouco cristalina, normalmente encontrada nas calcificações de cartilagem .

12. Na cartilagem articular, a apoptose dos condrócitos parece ter alguma relação com a calcificação.

13. A calcificação da cartilagem articular precede a formação de um centro secundário de ossificação, encontrado nos animais mais velhos.

5. Referências:

Anderson HC (1995) Molecular biology of matrix vesicles. Clin Orthop 34: 266-280

Barreto C, Albrecht RM, Bjorling DE, Horner JR, Wilsman NJ (1993) Evidence of the growth plate and the growth of long bones in juvenile dinosaurs. Science 262: 2020-2023

Bianco P, Cancedda FD, Riminucci M, Cancedda R (1998) Bone formation via Cartilage Models: The "bordeline chondrocytes". Matrix Biol 17: 185-192

Breur GJ, vanEnkevort BA, Farnum CE, Wilsman NJ (1991) Linear relationship between the volume of hypertrophic chondrocytes and the rate of longitudinal bone growth in growth plates. J Orthop Res 9: 348-359

Breur GJ, Farnum CE, Padgett GA, Wilsman NJ (1992) Cellular basis of decreased rate of longitudinal growth of bone in pseudoachondroplastic dogs. J Bone Jt Surg 74-A: 516-528

Bronckers ALJJ, Goei W, van Heerde WL, Dumont EAWJ, Reutelingsperger CPM, van den Eijnde SM (2000) Phagocytosis of dying chondrocytes by osteoclasts in the mouse growth plate as demonstrated by annexin-V labelling. Cell Tissue Res 301: 267-272

Buckwalter JA, Mower D, Ungar R, Schaeffer J, Ginsberg B (1986) Morphometric analysis of chondrocyte hypertrophy. J Bone Joint Surg 68-A: 243-255

Cancedda R, Cancedda FD, Castagnola P (1995) Chondrocyte differentiation. Int Rev Cytol 159: 265-359

Carvalho HF, Felisbino SL, (1999) The development of the pressure-bearing tendon in the bullfrog *Rana catesbeiana.* Anat Embryol 200: 55-64

Dell'Orbo C, Gioglio L, Quacci D (1992) Morphology of epiphyseal apparatus of a ranid frog. Histol Histopathol 7: 267-273

Dikson RG (1982) Ultrastruture of growth cartilage in the proximal femur of the frog, *Rana temporaria*. J Anat 135: 549-564

Elerbacher A, Filvaroff EH, Giltelman SE and Derynck R (1995) Toward a molecular understanding of skeletal development. Cell 80: 371-378

Felisbino SL, Carvalho HF (1999) The epiphyseal cartilage and growth of long bones in *Rana catesbeiana*. Tissue Cell 31: 301-307

Gardner E, Gray DJ (1970) The prenatal development of the human femur. Am J Anat 129: 121-140

Gentili C, Bianco P, Neri M, Malpeli M, Campanile G, Castagnola P, Cancedda R, Cancedda FD (1993) Cell proliferation, extracellular matrix mineralization, and ovotransferrin transient expression during in vitro differentiation of chick hypertrophic chondrocytes into osteoblast-like cells. J Cell Biol 122: 703-712

Gerstenfeld LC, Shapiro FD (1996) Expression of bone-specific genes by hypertrophic chondrocytes: Implications of the complex functions of the hypertrophic chondrocyte during endochondral bone development. J Cell Biochem 62: 1-9

Gibson G (1998) Active role of chondrocyte apoptosis in endochondral ossification. Microsc Res Tech 43: 191-204

Gibson GJ, Flint MH (1985) Type X collagen syntesis by chick sternal cartilage and its relationship to endochondral development. J Cell Biol 101: 277-284

Haines RW (1942) The evolution of epiphyses and of endochondral bone. Biol Rev 17: 267-292

Hashimoto S, Ochs RL, Rosen F, Quach J, McCabe G, Solan J, Seegmiller JE, Terkeltaub R, Lotz M (1998) Chondrocyte-derived apoptotic bodies and calcification of articular cartilage. Proc Natl Acad Sci USA. 95: 3094-3099

Hatori M, Klatte KJ, Teixeira CC, Shapiro IM (1995) End labelling studies of fragmented DNA in the avian growth plate: Evidence of apoptosis in terminally differentiated chondrocytes. J Bone Miner Res. 10: 1960-1968

Hunziker, E.B., Schenk, R.K and Cruz-Orive, L.M. 1987. Quantitation of chondrocyte performance in growth-plate cartilage during longitudinal bone growth. J Bone Joint Surg 69-A: 162-173

Hunziker EB, Schenk RK (1989) Physiological mechanisms adopted by chondrocytes in regulating longitudinal bone growth in rats. J Physiol 414: 55-71

Hunziker EB (1994) Mechanism of longitudinal bone growth and its regulation by growth plate chondrocytes. Microsc Res Tech 28: 505-519

Kim KM (1995) Apoptosis and calcification. Scannig Microsc 9: 1137-1178

Kirsch R, Nah HD, Shapiro IM, Pacifici M (1997) Regulated production of mineralization-competent matrix vesicles in hypertrophic chondrocytes. J Cell Biol 137: 1149-1160

Kwan API, Cummings CE, Chapman JA, Grant ME (1991) Macromolecular organization of chicken type X collagen in vitro. J Cell Biol 114: 597-604

Leboy PS, Vaias L, Uschmann B, Golub E, Adams SL, Pacifici M (1989) Ascorbic acid induces alkaline phosphatase, type X collagen, and calcium deposition in cultured chick chondrocytes. J Biol Chem 264: 17281-17286

Mopty SM, Cimarosti LO (1979) Estudio comparativo de la estructura histologica del femur de algunos anfibios. Acta Zool Lill 35: 263-268

Olsen BR (1995) Mutations in collagen genes resulting in metaphyseal and epiphyseal dysplasias. Bone 17: 45S-49S

Osdoby P, Caplan AI (1981) First bone formation in the developing chick limb. Develop Biol 86: 147-156

Poole AR (1991) The growth plate: Cellular physiology, cartilage assembly and mineralization. In: Hall BK, Newman SA (eds) Cartilage: Molecular aspects. CRC Press, Boca Raton, FL, pp 179-211

Roach HI, Erenpreisa J, Aigner T (1995) Osteogenic differentiation of hypertrophic chondrocytes involves asymmetric cell divisions and apoptosis. J Cell Biol 131: 483-493

Rosati R, Horan GSB, Pinero GJ, Garofalo S, Keene DR, Horton WA, Vuorio E, de Crombrugghe B, Behringer RR (1994) Normal long bone growth and development in type X collagen-null mice. Nature Genet 8: 129-135

Schmid TM, Linsenmayer TF (1983) Short chain (pro)collagen from aged endochondral chondrocytes. Biochemical characterization. J Biol Chem 258: 9504-9509

Silvestrini, G., Ricordi, M.E. and Bonucci, E. 1979. Resorption of uncalcified cartilage in the diaphysis of the chick embryo tibia. Cell Tissue Res 196: 221-235.

Wilsman NJ, Farnum CE, Green EM, Lieferman EM, Clayton MK (1996a) Cell cycle analysis of proliferative zone chondrocytes in growth plates elongating at different rates. J Orthop Res 14: 562-572

Wilsman NJ, Farnum CE, Lieferman EM, Fry M, Barreto C (1996b) Differential growth by growth plates as a function of multiple parameters of chondrocytic kinetics. J Orthop Res 14: 927-936

Zenmio M, Komiya S, Kawabata R, Sasaguri Y, Inoue A, Morimatsu M (1996) Morphological and biochemical evidence for apoptosis in the terminal hypertrophic chondrocytes of the growth plate. J Pathol 180: 430-433